

## Vortex state in a $d$ -wave superconductor

M. Franz, C. Kallin, and P. I. Soininen

*Department of Physics and Astronomy, McMaster University, Hamilton, Ontario, Canada L8S 4M1*

A. J. Berlinsky

*Brockhouse Institute for Materials Research, McMaster University, Hamilton, Ontario, Canada L8S 4M1*

A. L. Fetter

*Department of Physics, Stanford University, Stanford, California 94305*

(Received 15 September 1995)

We discuss the physics of the vortex state in a  $d$ -wave superconductor, using the phenomenological Ginzburg-Landau theory, where many unusual phenomena arise from the small admixture of the  $s$ -wave component induced by spatial variations in the dominant  $d$  wave. Properties of an isolated vortex and of the Abrikosov vortex lattice are studied by means of analytic and numerical methods. An isolated vortex has a considerable structure, with four “extra” nodes in the  $s$ -wave order parameter symmetrically placed around the core and an amplitude forming a four-lobe profile decaying as  $1/r^2$  at large distances. The supercurrent and magnetic-field distributions are also calculated. The Abrikosov lattice is in general oblique with the precise shape determined by the magnetic field and  $s$ - $d$  mixing parameter  $\epsilon_v$ . The magnetic-field distribution in the Abrikosov state has two nonequivalent saddle points resulting in the prediction of a double peak line shape in  $\mu$ SR and NMR experiments as a test of a  $d$ -wave symmetry. Detailed comparison is made with existing experimental data and experiments are proposed to test for the predicted effects.

### I. INTRODUCTION

After several years of debate there is growing agreement that the symmetry of the order parameter in the high- $T_c$  cuprate superconductors is not a conventional isotropic  $s$  wave, but has a more complicated structure involving nodes in the gap. Recent experiments sensitive to the phase of the order parameter<sup>1,2</sup> provide strong evidence for the  $d_{x^2-y^2}$  symmetry with lines of nodes along the  $|k_x|=|k_y|$  directions. Support for the  $d$ -wave symmetry also arises from specific heat measurements<sup>3</sup> and the recent observation of a nonlinear Meissner effect.<sup>4</sup> Photoemission studies,<sup>5</sup> Josephson interference,<sup>6</sup> and  $c$ -axis Josephson tunneling<sup>7</sup> experiments have been interpreted as being inconsistent with a pure  $d$ -wave order parameter. However, most of these inconsistencies can be reconciled by allowing for states of mixed symmetry.<sup>8</sup> In orthorhombic materials, such as Y-Ba-Cu-O (YBCO) and Bi-Sr-Ca-Cu-O (BiSCCO), if the dominant order parameter is  $d$  wave, a small  $s$  component will be present<sup>9</sup> even in a strictly uniform system. In tetragonal  $d$ -wave materials, which will be considered in this work, this  $s$ -wave component vanishes identically in the bulk; however it may be nucleated locally by perturbations which induce spatial variations of the  $d$ -wave order parameter,<sup>10,11</sup> e.g., by external magnetic fields, surfaces or impurities. In the present work we consider the vortex state of a  $d$ -wave superconductor which results from applying a uniform magnetic field parallel to the  $c$  axis of the superconductor. We study the properties of isolated vortices and of the Abrikosov vortex lattice, both of which differ in many aspects from those found in conventional superconductors, owing to the induced  $s$ -wave component. These effects will play an important role in transport properties of high- $T_c$  materials,

which in turn are crucial for all practical applications. Understanding the static properties of  $d$ -wave vortices is a first important step toward the description of the more complex dynamical effects in the presence of transport currents, surfaces, impurities, etc.

The problem of an isolated vortex line in a  $d$ -wave superconductor was first studied by Soininen, Kallin, and Berlinsky<sup>11</sup> who considered a simple microscopic lattice model for electrons with on-site repulsion and nearest neighbor attraction. The resulting Bogoliubov-de Gennes (BdG) equations were solved numerically on finite clusters to obtain the order parameter distribution for a single vortex. It was found that a substantial  $s$ -wave component is nucleated near the vortex core with opposite winding of phase relative to the  $d$  component,<sup>10</sup> and a distinct four-lobe shape of the amplitude. These results were interpreted with help of the phenomenological Ginzburg-Landau (GL) theory,<sup>12-14</sup> where the nonzero  $s$  is driven by a mixed gradient coupling to the  $d$  component. Ren, Xu, and Ting<sup>15</sup> later attempted a Gorkov-type derivation of the GL theory from a continuum mean field model of  $d$ -wave superconductivity and used the resulting free energy to discuss the qualitative properties of a single vortex. They obtained useful asymptotic expressions for the behavior of the order parameters in various regions of the vortex. Wang and MacDonald<sup>16</sup> investigated numerically the electronic excitations inside and outside the cores of  $s$ -wave and  $d$ -wave vortices using the self-consistent BdG equations. They found a distinctly different behavior of the  $T=0$  quasiparticle density of states in the core of the  $d$ -wave vortex compared to that in the  $s$ -wave core within the same model. Very recently Ichioka *et al.*<sup>17</sup> analyzed the structure of a  $d$ -wave vortex within the quasi-classical Eilenberger formalism. Their results appear to agree in every aspect with

the results of GL theory presented below and in an earlier letter.<sup>18</sup> While the properties of an isolated vortex are now relatively well understood, those of the vortex lattice have remained largely unexplored.<sup>19</sup>

Much of the work discussed above is based on a particular (effective) microscopic model of superconductivity. However there is presently no general agreement on the fundamental mechanism of pairing in the high- $T_c$  cuprates. A good alternative in such a situation is to study the phenomenological GL theory, which is based only upon general concepts related to symmetries of the system. Application of such theory to conventional ( $s$ -wave) superconductors has demonstrated its ability to predict virtually all of their phenomenological properties. In Sec. II, we review the GL theory appropriate for the  $d$ -wave superconductor, which involves both  $d$ -wave and an induced  $s$ -wave order parameter generated through the mixed gradient coupling. We discuss some of the general properties of this free energy and derive the corresponding GL differential equations as well as an expression for the supercurrent. In doing this, and throughout the entire paper, we restrict ourselves to the simple case of tetragonal symmetry, described by the point group  $D_4$ . Thus the results presented below are strictly applicable only to truly tetragonal cuprates (such as  $Tl_2Ba_2CuO_{6+d}$ ); however it is reasonable to expect that the more common class of orthorhombic materials will show at least qualitatively similar behavior.

Sections III and IV are devoted to the study of a single vortex and of the Abrikosov vortex lattice. Some of the results described here have been previously reported in a letter.<sup>18</sup> Here we offer a more comprehensive treatment of the problem, and we present a number of previously unpublished results. For the single vortex we first review known analytical results and complement these by several observations. We then carry out numerical integration of the GL equations for the single vortex geometry. In the region close to the vortex core our results confirm previous work within the BdG framework.<sup>11</sup> In particular we find the induced  $s$ -wave order parameter which has the expected four-lobe structure with minima along  $\pm x$ ,  $\pm y$  axes and maxima along the  $|x|=|y|$  diagonals, and the phase winding in the opposite sense relative to the  $d$  wave. Farther from the core the GL theory yields results that were inaccessible to the BdG treatment due to the cluster size limitations. At a distance of several coherence lengths from the core the winding number of the  $s$  wave changes from  $-1$  to  $+3$  resulting in four "extra" nodes in the  $s$ -wave order parameter symmetrically placed along the  $\pm x$ ,  $\pm y$  axes. Analysis of the asymptotic solutions shows that these nodes are necessarily present in the  $s$  component, whenever pure  $d$ -wave solutions are thermodynamically stable in the bulk. Our numerical work supports this conclusion. Quite generally the distribution of the  $d$  component, as well as the supercurrent and the magnetic field, exhibit a fourfold anisotropy, the magnitude of which is proportional to the relative magnitude of  $s$ .

As was mentioned above, the problem of the vortex lattice, which forms in magnetic fields close to the upper critical field  $H_{c2}$ , has not been previously addressed for a  $d$ -wave superconductor. In view of the fourfold anisotropy of individual vortices one may expect that the conventional triangular Abrikosov lattice<sup>20,21</sup> will be modified, especially

since, even in the absence of anisotropy, the difference in the free energy between triangular and square lattices is extremely small (less than 2%). Moreover, recent neutron scattering<sup>22</sup> and scanning tunneling microscopy (STM) (Ref. 23) experiments reveal an oblique vortex lattice in YBCO in strong magnetic fields. In Sec. IV we solve for the structure of the vortex lattice in the vicinity of  $H_{c2}$ . We generalize the classic Abrikosov<sup>20</sup> treatment to the  $d$ -wave case by first minimizing the quadratic part of the free energy using a Gaussian variational wave function, and then forming a periodic array of vortices from linear combination of these functions. We include the effects of the vector potential coupling self-consistently, thus improving upon our original calculation<sup>18</sup> which neglected these effects. The resulting vortex lattice is found to be oblique, with an angle between primitive vectors ranging from  $60^\circ$  to  $90^\circ$ , depending on the strength of the mixed gradient coupling and magnetic field and to a lesser extent on the other parameters in the GL free energy.

In Sec. V we summarize our results and discuss in some detail their relevance to the existing experimental data. We also propose experiments that might directly test some of our predictions.

## II. GINZBURG-LANDAU THEORY OF A SUPERCONDUCTOR WITH $d$ -WAVE PAIRING

The Ginzburg-Landau (GL) theory for a superconductor with  $d_{x^2-y^2}$  symmetry has been described by Joynt.<sup>12</sup> The free energy density is expressed in terms of two components of the order parameter,  $s(\mathbf{r})$  and  $d(\mathbf{r})$ , with appropriate symmetries, as follows:

$$f = \alpha_s |s|^2 + \alpha_d |d|^2 + \beta_1 |s|^4 + \beta_2 |d|^4 + \beta_3 |s|^2 |d|^2 + \beta_4 (s^{*2} d^2 + d^{*2} s^2) + \gamma_s |\vec{\Pi} s|^2 + \gamma_d |\vec{\Pi} d|^2 + \gamma_v [(\Pi_y s)^*(\Pi_y d) - (\Pi_x s)^*(\Pi_x d) + \text{c.c.}] + \hbar^2/8\pi. \quad (1)$$

Here  $\vec{\Pi} = -i\nabla - e^* \mathbf{A}/\hbar c$ , and we assume that  $d$  is a critical order parameter, i.e., we take  $\alpha_s = \alpha'(T - T_s)$  and  $\alpha_d = \alpha'(T - T_d)$  with  $T_s < T_d$ . The use of the same temperature derivative,  $\alpha'$ , for  $\alpha_s$  and  $\alpha_d$  is justified below. This also allows us to set  $\alpha' = 1$  in the subsequent analysis. We assume that  $\beta_1, \beta_2, \beta_3, \beta_4, \gamma_s$  and  $\gamma_d$  are all positive as it is suggested by a simple lattice model<sup>11</sup> and a Gorkov-type calculation within the continuum weak coupling theory.<sup>15</sup> We also choose  $\gamma_v$  to be positive throughout this work.<sup>24</sup> The parameters  $\gamma$  are related to the effective masses in the usual way, with  $\gamma_i = \hbar^2/2m_i^*$ , for  $i = s, d, v$ . We shall be interested in the case when pure  $d$ -wave state is stable in the bulk in the absence of perturbations, i.e., situations when  $|d| > 0, s = 0$ . The condition for such a state to be thermodynamically stable is<sup>11</sup>

$$\alpha_d < 0, \quad 2\beta_2 \alpha_s + (\beta_3 - 2|\beta_4|) |\alpha_d| > 0. \quad (2)$$

With a finite  $d$  component, the second transition temperature  $T_s$  will be renormalized by the fourth order invariants. In particular the transition to the state with finite bulk  $s$ -wave component will occur at

$$T_s^* = T_s - \frac{(\beta_3 - 2|\beta_4|)}{2\beta_2 - (\beta_3 - 2|\beta_4|)}(T_d - T_s). \quad (3)$$

Thus, even if the bare  $T_s$  is close to  $T_d$ , the true transition temperature  $T_s^*$  may be much lower. Moreover, when  $2\beta_2 - (\beta_3 - 2|\beta_4|) \leq 0$ , a second transition will never occur and we may conclude that the precise value of  $T_s$  is not very important for the physics.

There are various ways of interpreting  $f$ , some of which

$$f_b = \alpha_0(|v|^2 + |h|^2) + \epsilon(vh^* + hv^*) + \gamma_L(|\Pi_x h|^2 + |\Pi_y v|^2) + \gamma_T(|\Pi_y h|^2 + |\Pi_x v|^2) + \gamma_C[(\Pi_x h)(\Pi_x v)^* + (\Pi_y h)(\Pi_y v)^* + \text{c.c.}] + \beta(|h|^4 + |v|^4) + h^2/8\pi. \quad (4)$$

In Eq. (4),  $\alpha_0 = \alpha'(T - T_0)$ , and  $\epsilon$  stabilizes the relative phase of  $v$  and  $h$ . If  $\epsilon$  is positive, then a relative phase of  $\pi$  is stabilized, and the stable state has  $d$ -wave symmetry. If  $\epsilon < 0$ , then the quadratic terms in  $f_b$  are minimized when  $v$  and  $h$  have the same phase, giving a state with (extended)  $s$  symmetry. The first two coefficients of the gradient terms  $\gamma_L$  and  $\gamma_T$  involve derivatives along (e.g.,  $\Pi_y v$ ) and transverse (e.g.,  $\Pi_x v$ ) to the bond directions. In general, these two coefficients will be different. The fourth order terms, proportional to  $\beta$ , which are included in  $f_b$  are the terms which would arise in the mean field theory of  $XY$  spins. In general, a mean field theory for fermions will have other terms. However, it is instructive to consider the consequences of these simple fourth order terms, i.e.,  $|h|^4 + |v|^4$ .

The orthonormal transformation,  $s = (h + v)/\sqrt{2}$ ,  $d = (v - h)/\sqrt{2}$ , allows us to express the coefficients of Eq. (1) in terms of the coefficients in  $f_b$ . The results are

$$\alpha_s = \alpha_0 - \epsilon, \quad \alpha_d = \alpha_0 + \epsilon, \quad (5)$$

$$\beta_1 = \beta_2 = \beta_4 = \beta, \quad \beta_3 = 4\beta, \quad (6)$$

$$\gamma_s = (\gamma_L + \gamma_T)/2 + \gamma_C,$$

$$\gamma_d = (\gamma_L + \gamma_T)/2 - \gamma_C, \quad \gamma_v = (\gamma_L - \gamma_T)/2. \quad (7)$$

The statement that the same value of  $\alpha'$  occurs in  $\alpha_s$  and  $\alpha_d$  is equivalent to the statement that the temperature derivative of  $\epsilon$  is negligible in comparison to the temperature derivative of  $\alpha_0$ . If that is not the case, then this approximation is not valid. In what follows we shall adopt the above approximation for computational convenience, but we note that it is in no way essential for the conclusions of this work, and relaxing it only leads to small quantitative changes. The fourth order terms,  $|h|^4 + |v|^4$ , generate all of the terms in Eq. (1) with comparable magnitudes; in fact the resulting relative magnitudes of  $\beta_i$ 's are very close to the weak coupling values.<sup>15</sup> The mixed gradient term,  $\gamma_v$ , arises from the *difference* in the coefficients of the longitudinal and transverse gradient terms in the bond picture. Of course, this difference could be zero, but that is not expected on the basis of symmetry.

have been discussed by Joynt<sup>12</sup> and by Volovik.<sup>10</sup> Here we provide an interpretation in terms of nearest neighbor bond fields  $v(\mathbf{r})$  and  $h(\mathbf{r})$ . These fields describe the superconducting pairing amplitudes on the vertical ( $v$ ) and horizontal ( $h$ ) bonds of the square lattice representing the crystalline structure of the cuprate superconductor, and arise naturally in the simple mean field lattice models of superconductivity with on site repulsion and nearest neighbor attraction between electrons.<sup>11,25</sup> For tetragonal symmetry, the free energy  $f_b$  may be written in terms of these bond fields as follows:

To study the implications of the above free energy (1) for the structure of the isolated vortex line and the vortex lattice the first necessary step is to write down the field equations for the order parameters. These are obtained in the standard way by varying the free energy (1) with respect to conjugate fields  $d^*$  and  $s^*$ . We have

$$(\gamma_d \Pi^2 + \alpha_d)d + \gamma_v(\Pi_y^2 - \Pi_x^2)s + 2\beta_2|d|^2d + \beta_3|s|^2d + 2\beta_4 s^2 d^* = 0, \quad (8a)$$

$$(\gamma_s \Pi^2 + \alpha_s)s + \gamma_v(\Pi_y^2 - \Pi_x^2)d + 2\beta_1|s|^2s + \beta_3|d|^2s + 2\beta_4 d^2 s^* = 0. \quad (8b)$$

In a similar manner, one obtains the current density in the  $xy$  plane:

$$\mathbf{j} = \frac{e^* \hbar}{2m_d^*} [d^*(\vec{\Pi}d) + (\vec{\Pi}d)^*d] + \frac{e^* \hbar}{2m_s^*} [s^*(\vec{\Pi}s) + (\vec{\Pi}s)^*s] - \hat{x} \frac{e^* \hbar}{2m_v^*} [s^*(\Pi_x d) + (\Pi_x s)^*d + \text{c.c.}] + \hat{y} \frac{e^* \hbar}{2m_v^*} [s^*(\Pi_y d) + (\Pi_y s)^*d + \text{c.c.}]. \quad (9)$$

In carrying through the variational procedure it is necessary to impose appropriate boundary conditions for the superconductor-vacuum boundary. For our two component system these turn out to be

$$\mathbf{n} \cdot [\gamma_d \vec{\Pi}d + \gamma_v(\hat{y}\Pi_y s - \hat{x}\Pi_x s)] = 0, \quad (10a)$$

$$\mathbf{n} \cdot [\gamma_s \vec{\Pi}s + \gamma_v(\hat{y}\Pi_y d - \hat{x}\Pi_x d)] = 0, \quad (10b)$$

where  $\mathbf{n}$  is the unit vector normal to the surface. By combining the above two equations and comparing with the expression for the current density (9), one can easily deduce that

$$\mathbf{n} \cdot \mathbf{j}|_{\text{boundary}} = 0,$$

i.e., the normal component of supercurrent vanishes, as required on the superconductor-vacuum boundary. We also note that for the special case of a flat boundary along say the  $yz$  plane, conditions (10) acquire the simple form

$\Pi_x s = \Pi_x d = 0$ , which is analogous to the boundary condition in the usual one component system.

The above set of equations constitutes a complete Ginzburg-Landau theory for a superconductor with  $d_{x^2-y^2}$  pairing. This full theory is evidently too complicated for most practical purposes, and one must resort to approximations in order to obtain useful results. The rest of this paper is devoted to two such approximations valid in weak and strong magnetic fields.

### III. NEAR $H_{c1}$ : ISOLATED VORTEX LINE

When the applied magnetic field  $H$  is close to the lower critical field,  $H_{c1}$ , spacing between individual vortex lines is large and it is sufficient to consider structure of a single isolated vortex. As mentioned in the Introduction, a single vortex line in a  $d$ -wave superconductor exhibits rich and rather fascinating properties that have no analog in conventional superconductors with a single component order parameter. In the present section we discuss these properties in some detail. First we review the analytical results concerning the distribution of the order parameter, supercurrent and magnetic field in various regions of the vortex. Second, we carry out an explicit numerical integration of the GL equations for the single vortex geometry to confirm and complement these analytic solutions.

#### A. Analytic solutions

As is appropriate in the case of high- $T_c$  cuprate superconductors, we shall consider strongly type-II materials, in which magnetic fields vary over length scale  $\lambda$  that is much larger than the relevant coherence length  $\xi$  over which significant variations of the order parameter can occur. In what follows we focus only on situations where magnetic field is parallel to the  $c$  axis of the superconductor.

For the problem of a single vortex line it will be convenient to work in the cylindrical gauge expressed in the usual polar coordinates  $(r, \varphi)$ ,

$$\mathbf{A} = \hat{\varphi} A(r), \quad (11)$$

with

$$A(r) = \frac{1}{r} \int_0^r r' h(r') dr'. \quad (12)$$

By adopting this particular gauge we restrict ourselves to magnetic fields  $\mathbf{h}(\mathbf{r}) = \hat{z} h(r)$  that have no angular dependence. While this is clearly not exact for the  $d$ -wave vortex, we shall see that quite generally the part of  $\mathbf{h}$  that is not rotationally invariant is small and can thus be computed as a perturbative correction to (11).

Let us first look at the behavior of the order parameter near the center of the vortex, as  $r \rightarrow 0$ . In the relevant region where  $r \ll \lambda$  the magnetic field can be treated as constant,  $h = h(0) \equiv h_0$  and the vector potential becomes

$$A(r) = \frac{1}{2} h_0 r. \quad (13)$$

For the singly quantized vortex  $h_0$  can be roughly estimated by requiring that the area  $\sim \pi \lambda^2$  contains magnetic flux equal to a single flux quantum  $\Phi_0 = hc/e^*$ . This gives

$h_0 \approx \Phi_0 / \pi \lambda^2$ . The problem is now to find simultaneous solutions to the two GL equations (8) for  $s$  and  $d$ , to leading order as  $r \rightarrow 0$ . Qualitatively it is clear that at the core ( $r=0$ ) both  $d$  and  $s$  vanish. Moving outward from the core, the amplitude of  $d$  increases and generates nonzero  $s$  via the mixed gradient coupling. Around  $r = \xi_d \equiv \sqrt{\gamma_d / |\alpha_d|}$  the amplitude of  $d$  starts to level off, attaining eventually its bulk value  $d_0 \equiv \sqrt{|\alpha_d| / 2\beta_2}$ , which causes  $|s|$  to reach a maximum and then decrease to 0 as  $r \rightarrow \infty$ . This qualitative picture suggests that in order to study the leading order behavior we may first solve Eq. (8a) for  $d$  assuming  $s=0$ , and then obtain the leading behavior of  $s$  from Eq. (8b). With this assumption Eq. (8a) becomes

$$(\alpha_d + \gamma_d \Pi^2) d + 2\beta_2 |d|^2 d = 0, \quad (14)$$

which is identical to the GL equation for the conventional one component superconductor. The asymptotic solution to this equation near the core is well known to be<sup>26</sup>

$$d(r, \varphi) \approx (d_1 r + d_3 r^3) e^{i\varphi}, \quad (15)$$

where constant  $d_3$  is given by

$$d_3 = -\frac{d_1}{8\xi_d^2} [1 + 2\pi\xi_d^2 h_0 / \Phi_0], \quad (16)$$

and  $d_1$  can be obtained by full integration of Eq. (14). Note that ordinarily only the leading dependence  $d(r, \varphi) \approx d_1 r e^{i\varphi}$  is quoted; however, it turns out that in our case the term  $d_3 r^3 e^{i\varphi}$  is necessary to obtain a consistent expression for  $s(r, \varphi)$ . In Eq. (16) the factor  $\Phi_0 / 2\pi\xi_d^2$  dividing  $h_0$  is of the order of the zero temperature upper critical field  $H_{c2}(0)$ . Since we are interested in the region close to  $H_{c1}$ , we have  $h_0 \ll H_{c2}$  and in what follows we shall consistently neglect terms  $\sim h_0 / H_{c2}$  compared to unity. With this simplification Eq. (16) becomes

$$d_3 \approx -d_1 / 8\xi_d^2. \quad (17)$$

The leading behavior of  $s(r, \varphi)$  now can be obtained from the linearized version of Eq. (8b) which reads

$$(\alpha_s + \gamma_s \Pi^2) s + \gamma_v (\Pi_y^2 - \Pi_x^2) d = 0, \quad (18)$$

by substituting for  $d$  from Eq. (15). Evaluating the action of the  $(\Pi_y^2 - \Pi_x^2)$  operator in polar coordinates gives

$$(\Pi_y^2 - \Pi_x^2) d(r, \varphi) = -\left(\frac{e^* h_0}{\hbar c}\right) d_1 r e^{-i\varphi} + d_3 r (3e^{-i\varphi} - e^{3i\varphi}), \quad (19)$$

which suggests that the  $s$  component is of the form

$$s(r, \varphi) = s_1 r e^{-i\varphi} + s_3 r^3 e^{3i\varphi}. \quad (20)$$

Comparing the coefficients in front of different phase factors and again neglecting terms  $\sim h_0 / H_{c2}(0)$ , we obtain

$$s_1 = \frac{3}{8} \left( \frac{\gamma_v}{\alpha_s \xi_d^2} \right) d_1, \quad (21)$$

and, to the same order,  $s_3 = 0$ .

In summary, the leading order behavior of the order parameter near the core is

$$d(r, \varphi) = d_1 r e^{i\varphi}, \quad (22a)$$

$$s(r, \varphi) = \frac{3}{8} \left( \frac{\gamma_v}{\alpha_s \xi_d^2} \right) d_1 r e^{-i\varphi}. \quad (22b)$$

The most interesting feature of this result is the opposite winding of the  $s$ -wave component relative to  $d$ . This was pointed out by Volovik<sup>10</sup> based on a general symmetry argument. The solution of the form (22) was also derived by Ren *et al.*,<sup>15</sup> however, the explicit form of the prefactor in the  $s$  component is a result of this work. Knowledge of this prefactor will allow us to give a simple but accurate estimate of the maximum  $s$ -wave amplitude,  $s_{\max} \equiv \max(|s|)$ , induced in the vicinity of the vortex core. In view of the fact that far outside the core  $s$  decays algebraically with  $r$  (see below), such an estimate is quite important for the assessment of the relative strength of the induced  $s$ -wave component and the various phenomena that its presence may lead to. The estimate is based on the assumption that near the core  $d$  and  $s$  rise over approximately the same length scale  $\sim \xi_d$ . In particular if we assume that at  $r = \xi_d$  the amplitude of  $d$  is approximately half of its bulk value<sup>26</sup>  $d_0$ , from Eq. (22a) we have  $\xi_d d_1 \approx d_0/2$ . Assuming further that  $|s|$  attains its maximum also around  $r = \xi_d$  we arrive at the following estimate:

$$\frac{s_{\max}}{d_0} \approx \frac{3}{16} \frac{\gamma_v}{\alpha_s \xi_d^2}. \quad (23)$$

A similar estimate was given previously by us,<sup>18</sup> based on a simple argument involving the competition between the mixed gradient term and other second order invariants in the free energy. This argument gave the correct functional dependence on the GL parameters, however it missed the numerical prefactor  $3/16 = 0.1875$ , which is important when investigating the quantitative properties of the above solution. Comparison to the numerical results (see the following subsection) shows that the above estimate (23) is correct to within about 20%, as long as  $s_{\max} < d_0/4$ . When  $s_{\max}$  becomes larger, the asymptotic solution (22) is no longer justified since the condition  $|s| \ll |d|$  is violated and our perturbative approach starts to break down.

A noteworthy consequence of Eq. (23) is the temperature dependence of  $s_{\max}$  near  $T_d$ . If we recall that close to  $T_d$  we have  $d_0 \sim \sqrt{1 - T/T_d}$  and  $\xi_d \sim 1/\sqrt{1 - T/T_d}$ , it follows that

$$s_{\max} \sim (1 - T/T_d)^{3/2}. \quad (24)$$

Faster decay of the  $s$  component near  $T_d$  compared to  $d$  is a direct consequence of the fact that as a noncritical order parameter the former is driven by the spatial variations of the latter.<sup>27</sup> Thus, sufficiently close to  $T_d$ , the  $s$  component will always be negligible compared to  $d$ , and in many aspects a  $d$ -wave superconductor will behave very much like a conventional single component superconductor. Equation (24) also self-consistently justifies the above perturbative solution of the GL equations near the core which assumes  $|s|$  to be small compared to  $|d|$ ; since  $s_{\max}/d_0 \sim (1 - T/T_d)$ , the condition  $|s| \ll |d|$  will be always fulfilled sufficiently close to  $T_d$ .

The supercurrent and the local magnetic field near the vortex core can be calculated from Eq. (9) using the order parameters given by Eq. (22). We obtain, to leading order in  $r$ ,

$$\mathbf{j}_s = d_1^2 \frac{2\gamma_d e^*}{\hbar} \left[ 1 - \left( \frac{3}{8} \frac{\gamma_v}{\alpha_s \xi_d^2} \right)^2 \right] \hat{\varphi} r, \quad (25)$$

$$\mathbf{h} = \hat{z} \left\{ h_0 - d_1^2 \frac{4\pi\gamma_d e^*}{c\hbar} \left[ 1 - \left( \frac{3}{8} \frac{\gamma_v}{\alpha_s \xi_d^2} \right)^2 \right] r^2 \right\}. \quad (26)$$

Expression (25) for the supercurrent shows explicitly that the  $s$  component with opposite winding of the phase relative to  $d$  in fact *diminishes* the total supercurrent, resulting in weaker shielding of the external magnetic field compared to the conventional superconductor.

We next consider the region outside the core,  $\xi_d \ll r \ll \lambda$ . We shall assume that in this region  $d$  has already reached its limiting form

$$d(r, \varphi) = d_0 e^{i\varphi}. \quad (27)$$

Because of the condition  $r \ll \lambda$ , the magnetic field can still be treated to a reasonable approximation as constant, and the vector potential is thus given by Eq. (13). It is, however, easy to show that coupling to the latter can be ignored in this region. In particular, rewriting all the relevant operators in polar cylindrical coordinates, one can easily show that for  $d(r, \varphi)$  given by (27) it holds that  $\Pi^2 d(r, \varphi) = d_0 r^{-2} (-1 + r^2/\lambda^2)^2$ . Clearly, the second term in the brackets (which originates from the vector potential  $\mathbf{A}$ ) can be safely ignored with respect to unity, since, by assumption,  $r/\lambda \ll 1$ . With some effort, one can demonstrate that the vector potential is also negligible in the terms  $(\Pi_y^2 - \Pi_x^2)d(r, \varphi)$ .

The problem of finding the asymptotic solution outside the core region reduces to solving Eq. (8b) for  $s(r, \varphi)$  with  $d$  given by (27) and  $\mathbf{A} = 0$ , and the additional assumptions that  $|s| \ll |d|$  and  $|\nabla s| \ll |\nabla d|$ . These allow one to consider only the linearized equation in which the relevant terms are

$$\gamma_v (\partial_x^2 - \partial_y^2) d + \alpha_s s + \beta_3 |d|^2 s + 2\beta_4 d^2 s^* = 0. \quad (28)$$

In polar coordinates,

$$(\partial_x^2 - \partial_y^2) d_0 e^{i\varphi} = \frac{1}{2r^2} (3e^{3i\varphi} - e^{-i\varphi}) d_0, \quad (29)$$

suggesting that the solution to Eq. (28) is of the form

$$s(r, \varphi) = \frac{1}{r^2} (f_1 e^{-i\varphi} + f_3 e^{3i\varphi}). \quad (30)$$

Substitution in Eq. (28) then gives

$$f_1 = \frac{1}{2} \gamma_v d_0 \frac{(\alpha_s + \beta_3 d_0^2) + 6\beta_4 d_0^2}{(\alpha_s + \beta_3 d_0^2)^2 - 4(\beta_4 d_0^2)^2}, \quad (31)$$

$$f_3 = -\frac{1}{2} \gamma_v d_0 \frac{3(\alpha_s + \beta_3 d_0^2) + 2\beta_4 d_0^2}{(\alpha_s + \beta_3 d_0^2)^2 - 4(\beta_4 d_0^2)^2}. \quad (32)$$

Asymptotic solution of this form was obtained by Ren *et al.*<sup>15</sup> From the knowledge of the order parameters

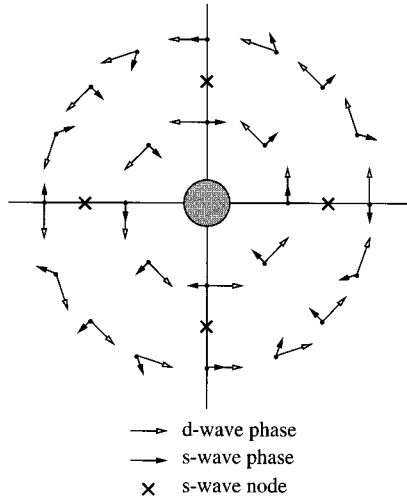


FIG. 1. Schematic diagram of phases  $\theta_d$  and  $\theta_s$  of the two components of the order parameter in the two asymptotic regions close to and far from the vortex core, as determined from Eqs. (22b) and (30). Note that this diagram is more complete than the similar one published in Ref. 11 in that it includes the region outside the core. The present diagram also differs from that in Ref. 15 which shows (we believe incorrectly) the  $s$  component with opposite overall sign outside the core.

$d(r, \varphi)$  and  $s(r, \varphi)$  one can compute the corresponding distributions of the supercurrent and the magnetic field. In order to do this consistently, one has to include corrections  $\sim 1/r^2$  to the  $d$  component [such as were neglected in Eq. (27)], as these are needed to insure that the continuity equation  $\nabla \cdot \mathbf{j} = 0$  is satisfied. The resulting formulas can be found in Ref. 15.

There are two important physical consequences of Eq. (30). First, the slow algebraic decay of the  $s$  component outside the core region means that asymptotically in the presence of a vortex, the superconductor is not in a pure  $d$ -wave state, rather there is a small  $s$ -wave admixture with angle dependent relative phase. As a result, fermionic excitations will be gapped in this region. As demonstrated below, only at the length scale set by the penetration depth is the  $s$  component cut off exponentially and a pure  $d$ -wave state is established.

A second interesting property of the  $s$ -wave component can be obtained by comparing the two solutions inside and outside the core. Inside the core Eq. (22b) implies that the winding number<sup>28</sup> of the  $s$  component is  $-1$ . The situation outside the core is slightly more complex, but near  $T_d$  it holds that  $f_3 \approx -3f_1$  [cf. Eqs. (31) and (32) in the limit  $d_0 \rightarrow 0$ ]. Thus the phase factor  $e^{3i\varphi}$  in Eq. (30) will dominate the behavior of  $s(r, \varphi)$  and the winding number far outside the core will be  $+3$ . For an analytic function the winding number is a conserved topological quantity which can be changed only by the presence of a node. This forces us to conclude that four additional positive vortices must exist outside the core in the  $s$  component.<sup>18</sup> These ‘‘extra’’ vortices (or nodes) are a consequence of the topological constraints imposed on the relative phases of  $s$  and  $d$  by the structure of the GL equations (8). Behavior of the phases  $\theta_s$  and  $\theta_d$  is schematically depicted in Fig. 1, for the two asymptotic regions as given by Eqs. (22), (27), and (30). By inspection of

the figure one may conclude that the four extra vortices are symmetrically placed on  $\pm x$  and  $\pm y$  axes, since the  $s$  component apparently changes sign along these directions. Finally we note that there are no extra nodes in the  $d$  component and that the total magnetic flux associated with one vortex line (consisting of 1  $d$ -wave node and 5  $s$ -wave nodes) is equal to one flux quantum; there is no additional flux associated with the extra  $s$ -wave nodes.

We have argued above that the unusual nodal structure of the  $d$ -wave vortex exists at temperatures close to  $T_d$ . It can be shown, however, that our argument has much wider validity. It is a simple matter to demonstrate that a complex function of the form  $g(\varphi) = ae^{-i\varphi} - be^{3i\varphi}$  with  $a, b > 0$ , will have winding number  $+3$  for  $b > a$  (and  $-1$  for  $b < a$ ). Applying this criterion to  $s(r, \varphi)$  given by Eq. (30) and with help of relations (31) and (32), one obtains the following inequality:

$$3(\alpha_s + \beta_3 d_0^2) + 2\beta_4 d_0^2 > (\alpha_s + \beta_3 d_0^2) + 6\beta_4 d_0^2, \quad (33)$$

as a requirement for the winding number  $+3$  outside the core. Upon expressing  $d_0^2$  as  $|\alpha_d|/2\beta_2$  and rearranging, one finds that this inequality coincides with the stability condition (2). It therefore follows that for all combinations of GL parameters consistent with stable  $d$ -wave state, the asymptotic winding number of  $s$  outside the core is  $+3$  and the non-trivial nodal structure described above exists. We may conclude that the structure of the vortex core in a  $d$ -wave superconductor is *inherently* much more complicated than that of a conventional vortex. This statement is valid over the entire range of temperatures in which the GL theory is applicable, in magnetic fields weak enough so that the vortex line can be considered isolated. Very recently, the existence of the extra nodes has been confirmed by Ichioka *et al.*,<sup>17</sup> who investigated the distribution of order parameters near the vortex using the quasi-classical Eilenberger equations. On the other hand, however, recent numerical computations within the GL theory by Xu *et al.*<sup>29</sup> failed to find evidence for this effect. One possible reason for this apparent discrepancy might be that Xu *et al.* present their results for a Ginzburg-Landau ratio  $\kappa = 2$  (i.e., weak type-II superconductor). The topological arguments in favor of extra vortices presented above only apply to the case of strong type-II superconductors ( $\kappa \gg 1$ ) which is relevant to the high- $T_c$  cuprates. It would be most interesting to see if evidence for the nontrivial vortex structure can be established in an experiment.

Finally we shall consider the region outside the core for  $r \gg \lambda$ . In this region we may still assume the asymptotic form (27) for  $d(r, \varphi)$ , but we can no longer treat the magnetic field as constant. Taking into account the fact that  $|s| \ll |d|$  in this region, we obtain the usual London equation for the vector potential, which in the cylindrical gauge (11) reads

$$\nabla^2 \mathbf{A} = -\frac{1}{\lambda^2} \left( \mathbf{A} - \frac{\Phi_0}{2\pi r} \hat{\varphi} \right). \quad (34)$$

The asymptotic solution to this equation for  $r \gg \lambda$  is

$$\mathbf{A} = \frac{\Phi_0}{2\pi\lambda} \left[ \frac{\lambda}{r} - \left( \frac{\pi\lambda}{2r} \right)^{1/2} e^{-r/\lambda} \right] \hat{\varphi}, \quad (35)$$

which gives the usual exponentially decaying magnetic field far from the vortex.<sup>26</sup> Using the vector potential given by (35) one can solve for  $s(r, \varphi)$  from Eq. (8b). The result, to the leading order in  $(r/\lambda)$ , is

$$s(r, \varphi) = \left( \frac{\pi \lambda}{2 r} \right)^{1/2} e^{-r/\lambda} (s_1 e^{-i\varphi} + s_3 e^{3i\varphi}), \quad (36)$$

with

$$s_1 = -s_3 = \frac{1}{2\lambda^2} \frac{\gamma_v d_0}{\alpha_s + (\beta_3 - 2\beta_4) d_0^2}. \quad (37)$$

Thus, as expected, the  $s$ -wave component will be exponentially small beyond distances from the core in excess of  $\lambda$ , and on these large length scales the  $d$ -wave superconductor will behave as a conventional single component type-II material. Equations (36) and (37) also show that to leading order, the total winding number of  $s(r, \varphi)$  remains undetermined (see the discussion of winding above). However, upon computing higher order terms in  $(r/\lambda)$  one finds that the winding number in this region remains  $+3$ , so that no additional nodes are required by topology outside the core region. If additional nodes do exist, their total winding must add to zero.

### B. Numerical results

The analytic results presented in the preceding subsection establish rich and complex structure of the vortex line in a  $d$ -wave superconductor; however, owing to the rather complex structure of the underlying GL equations (8) the analytic treatment is restricted to limiting cases where certain small parameters can be identified. Consequently, the information such a treatment provides is mainly of qualitative nature. In order to study the problem in more detail, we have integrated the GL equations numerically. Besides confirming the above analytic predictions, the numerical approach is capable of addressing the behavior of the order parameter at length scales comparable to  $\xi_d$ , where the analytic approach is difficult. In particular we will be most interested in the detailed behavior of the  $s$  component near the core, focusing on its exotic nodal structure that was predicted by topological arguments.

In order to arrive at a truly selfconsistent numerical solution, one should in principle complement the GL equations (8) by the Maxwell equation  $\nabla \times \mathbf{h}_s = (4\pi/c)\mathbf{j}$  and include the induced magnetic field  $\mathbf{h}_s$  in the total vector potential  $\mathbf{A}$ . However, as we are mostly interested in the region near the core ( $r \ll \lambda$ ), it is permissible to neglect these screening effects and indeed the coupling to the vector potential altogether, provided that we impose correct boundary conditions for a single vortex geometry (see below). Neglecting the vector potential leads to a significant simplification of the problem. Physically this corresponds to the extreme type-II limit,  $\lambda/\xi \rightarrow \infty$ . For a realistic system where  $\lambda/\xi$  is finite (but large), ignoring the vector potential coupling is equivalent to neglecting terms  $\sim (r/\lambda)^2$  compared to unity [see discussion following Eq. (27)].

With the vector potential absent from the GL equations it is convenient to introduce a set of dimensionless quantities such that  $\alpha_s$  is measured in units of  $|\alpha_d|$ ,  $\beta$  parameters in

units of  $2\beta_2$ ,  $s$  and  $d$  in units of the bulk  $d$ -wave gap  $d_0$ , and all the lengths in units of  $\xi_d$ . This allows one to write the GL equations (8) in the following simple dimensionless form:

$$-(\nabla^2 + 1)d + \epsilon_v (\partial_x^2 - \partial_y^2)s + |d|^2 d + \beta_3 |s|^2 d + 2\beta_4 s^2 d^* = 0, \quad (38a)$$

$$-(\nabla^2 - \alpha_s)s + \epsilon_v (\partial_x^2 - \partial_y^2)d + 2\beta_1 |s|^2 s + \beta_3 |d|^2 s + 2\beta_4 d^2 s^* = 0, \quad (38b)$$

where  $\epsilon_v = \gamma_v/\gamma_d$  and we have set  $\gamma_s = \gamma_d$ . On physical grounds [cf. Eq. (7)] we do not expect  $\gamma_s$  and  $\gamma_d$  to differ dramatically; and we have verified that allowing  $\gamma_s \neq \gamma_d$  does not have a significant effect on the solutions.

We have integrated Eqs. (38) numerically on a rectangular  $N \times N$  domain for the boundary conditions appropriate for a single vortex:

$$d|_{\text{boundary}} = d_0 e^{i\varphi}, \quad s|_{\text{boundary}} = 0. \quad (39)$$

We used an iterative Newton's algorithm as described in Ref. 30. At each step of iteration the conjugate gradient method<sup>31</sup> was used to solve the resulting system of linear equations.

Results of our numerical analysis indeed confirm all of the qualitative features found by the analytic considerations of the preceding subsection. Figure 2 shows the behavior of the  $d$ - and  $s$ -wave amplitudes near the center of the vortex, with parameters described in the figure caption. The resulting amplitude of the  $s$  component for this particular parameter configuration was  $s_{\text{max}} \approx 0.024d_0$ , in reasonable agreement with the estimate (23) which gives  $0.01875d_0$ . A domain size of  $N=201$  was used in the numerical integration, encompassing a physical region of the size  $L \approx 20\xi_d$ . In Fig. 2 only the central ( $121 \times 121$ ) region is displayed, where the boundary effects are expected to be strongly suppressed (the numerical solution was in fact well behaved all the way to the boundary of the system). As expected for this relatively weak admixture of the  $s$  component, the amplitude of  $d$  has almost perfect circular symmetry. The amplitude of  $s$  is nearly circular in the inner core of the vortex and it shows marked fourfold anisotropy outside the core, in accordance with the asymptotic solutions (22b) and (30). Four symmetrically placed maxima along diagonals and four nodes along  $\pm x$  and  $\pm y$  are visible in the contour plot. To see these more clearly we show in Fig. 3 the amplitudes of the  $s$ -wave component along  $x$ -axis and a  $x=y$  diagonal. A node close to  $x=3\xi_d$  is clearly visible, which is nothing else than one of the four extra vortices. The figure also confirms the linear behavior of  $|s|$  and  $|d|$  near the origin and the fact that both rise on approximately same length scale  $\xi_d$ . One can also see the  $1/r^2$  decay of  $|s|$  outside the core region, where  $|d|$  is constant.

Figure 4 shows the superconducting phases  $\theta_d$  and  $\theta_s$  of the two components of the order parameter. While the distribution of  $\theta_d$  looks very much like that of conventional singly quantized vortex, the distribution of  $\theta_s$  is clearly more complicated. In particular the opposite winding of the phase near the core and four positive vortices along the  $\pm x$ ,  $\pm y$  axes are clearly distinguishable. Comparison to Fig. 1 shows that

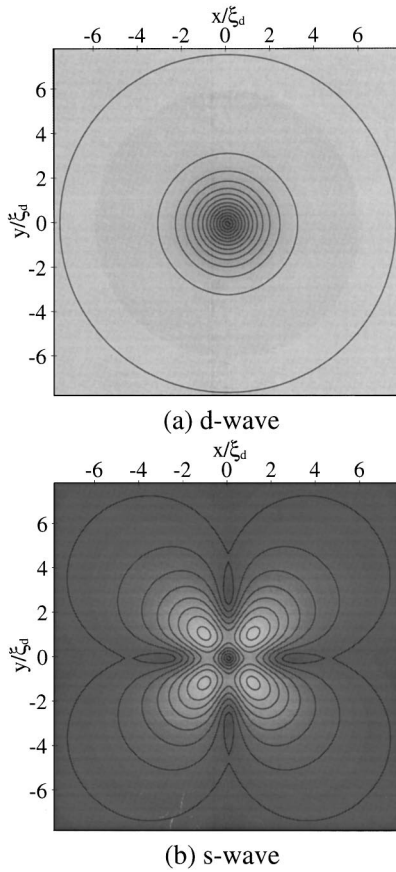


FIG. 2. Contour plot of the amplitudes of the (a)  $d$ -wave and (b)  $s$ -wave components of the order parameter as determined by numerical integration of the GL equations (38). The GL parameters used for the plot are  $\gamma_s = \gamma_d = \gamma_v$ ,  $\alpha_s = 10|\alpha_d|$ ,  $\beta_1 = \beta_3 = 0$ , and  $\beta_4 = 0.5\beta_2$ . The lightest regions of the diagram correspond to the largest amplitudes. The scale is in units of the  $d$ -wave coherence length  $\xi_d$ .

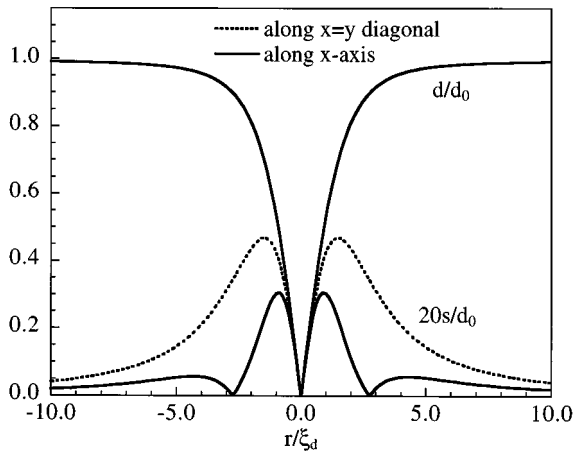


FIG. 3. Amplitude of the  $d$ -wave and the  $s$ -wave component along the  $x$  axis (solid line) and along the diagonal  $x=y$  (dotted line) normalized to the bulk value  $d_0$  (the  $s$  component is scaled by a factor 20 for clarity). The parameters used are the same as in Fig. 2. The  $d$  component is almost completely isotropic for this case so that the two cuts are indistinguishable.

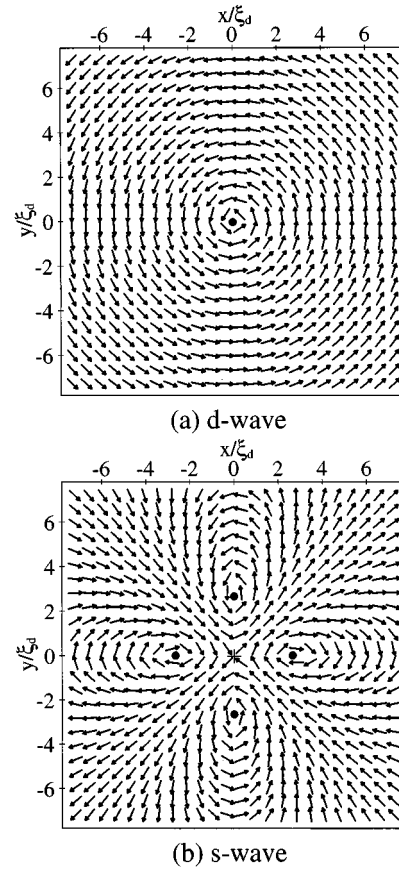


FIG. 4. The angle of arrow with respect to the horizontal  $x$  axis represents the phase of the (a)  $d$ -wave and (b)  $s$ -wave components of the order parameter. Solid dots represent positive vortices, “+” symbol represents negative vortex. The parameters used are the same as in Fig. 2.

our numerical results are again in complete agreement with the analytical predictions summarized in the preceding subsection.

The important quantity that determines the nature of excitations in the vicinity of the vortex line is the relative phase  $\Delta\theta \equiv \theta_s - \theta_d$ . We plot  $\Delta\theta$  in Fig. 5. Over much of the region

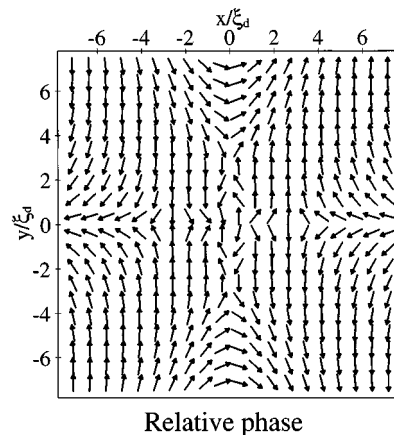


FIG. 5. The angle of arrow with respect to the horizontal  $x$  axis represents the relative phase  $\Delta\theta = \theta_s - \theta_d$  of the two components of the order parameter, for the same parameters as in Fig. 2.

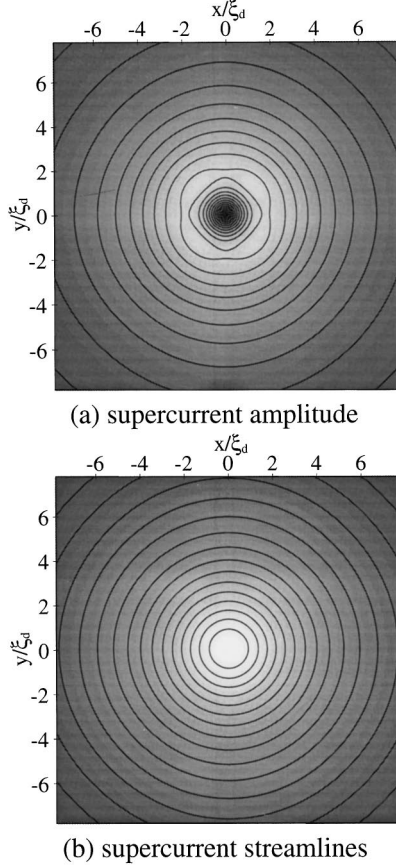


FIG. 6. Contour plot of (a) supercurrent amplitude (b) supercurrent streamlines (which coincide with the lines of constant magnetic field), for the same parameters as in Fig. 2.

the relative phase is  $\Delta\theta = \pm\pi/2$ , resulting in a  $d \pm is$  state that has minimum gap equal to  $|s|$ . This is a direct consequence of the fact that  $\beta_4 > 0$  in the free energy (1). However, the phase difference cannot be equal to  $\pm\pi/2$  over the entire area since this would be incompatible with the topological constraints that require opposite winding of the two components near the core. Thus narrow domain walls appear along the  $\pm x$ ,  $\pm y$  axes, where  $\Delta\theta$  changes rapidly. This result is in agreement with the microscopic treatment of Soinenen *et al.*<sup>11</sup> within the Bogoliubov–de Gennes theory. However since the complexity of this formalism did not allow one to extend the calculations to sufficient distances from the core, the extra vortices were originally not found. The present GL theory, being inherently simpler allows us to study larger clusters. As one moves further out from the core, domain walls abruptly end at the cores of the four  $s$ -wave vortices and  $\Delta\theta$  starts to vary more slowly while being still locked to  $\pm\pi/2$  over large areas.

Supercurrent  $\mathbf{j}$  produced by the above order parameter distribution, computed numerically from Eq. (9), is shown in Fig. 6. Panel (a) shows the distribution of the magnitude  $|\mathbf{j}|$  while panel (b) displays streamlines of the vector field  $\mathbf{j}$ . Note that because of the Ampère’s law  $\nabla \times \mathbf{h}_s = (4\pi/c)\mathbf{j}$ , the latter is equivalent to the lines of constant magnetic field given by the supercurrent, and thus Fig. 6(b) also gives the distribution of the spatially varying component of the screening field.

In addition to the particular case described above we have

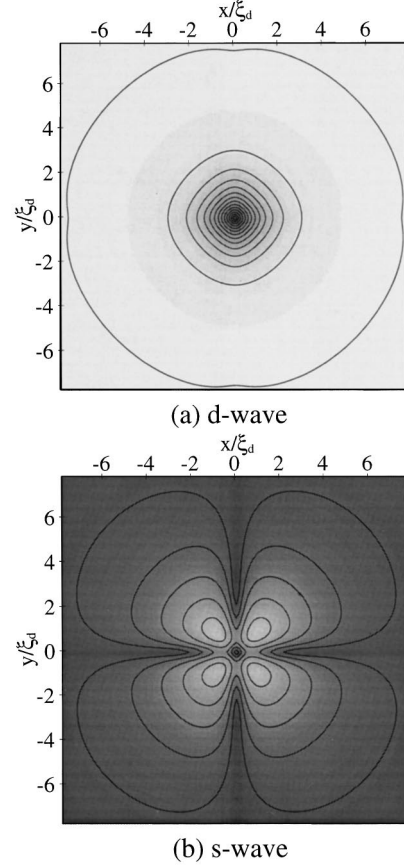


FIG. 7. Contour plot of the amplitudes of (a)  $d$ -wave and (b)  $s$ -wave components of the order parameter for a different set of GL parameters:  $\gamma_s = \gamma_d = \gamma_v$ ,  $\alpha_s = 1.4|\alpha_d|$ ,  $\beta_1 = \beta_2 = \beta_3 = \beta_4$ .

numerically studied a large number of other parameter combinations. All show similar behavior. The feature that changes between different configurations is the relative magnitude of the  $s$  component, which is, as we have explicitly verified, well described by Eq. (23). The larger the ratio  $s_{\max}/d_0$ , the more anisotropic the  $d$ -wave component becomes and along with it the distribution of supercurrent and induced magnetic field. As an example of such a case we show amplitudes of  $s$  and  $d$  in Fig. 7, for the particular parameter combination that yields  $s_{\max} \approx 0.15d_0$ . The relevant supercurrent distributions is plotted in Fig. 8.

#### IV. NEAR $H_{c2}$ : STRUCTURE OF THE VORTEX LATTICE

In what follows we present our treatment of the vortex lattice problem. In general we follow the path outlined by Abrikosov,<sup>20</sup> with necessary modifications that arise from the presence of two order parameters in the free energy.

##### A. Linearized GL equations and their variational solution

In the vicinity of the upper critical field  $H_{c2}$  the amplitudes of the order parameters are small, and the essential physics is contained in the linearized field equations that are obtained from (8) by neglecting the nonlinear terms:

$$(\gamma_d \Pi^2 + \alpha_d)d + \gamma_v(\Pi_y^2 - \Pi_x^2)s = 0, \quad (40a)$$

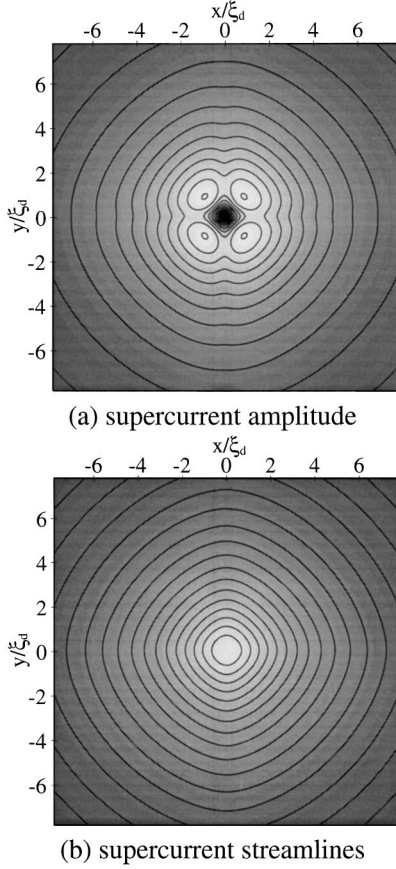


FIG. 8. Contour plot of (a) supercurrent amplitude (b) supercurrent streamlines (which coincide with the lines of constant magnetic field), for the same parameters as in Fig. 7.

$$(\gamma_s \Pi^2 + \alpha_s)s + \gamma_v(\Pi_y^2 - \Pi_x^2)d = 0. \quad (40b)$$

Formally this corresponds to the expansion to leading order in the small parameter  $(H_{c2} - H)/H_{c2}$ . The gauge invariant gradient  $\vec{\Pi}$  can be separated into two pieces,

$$\vec{\Pi} = \vec{\Pi}_0 + \vec{\Pi}_s \equiv (-i\nabla - e^* \mathbf{A}_0 / c\hbar) - e^* \mathbf{A}_s / c\hbar, \quad (41)$$

where  $\mathbf{H} = \nabla \times \mathbf{A}_0$  corresponds to the uniform applied field, and  $\mathbf{h}_s = \nabla \times \mathbf{A}_s$  is the screening field induced by the supercurrent  $\mathbf{j}_s$  in the sample, given by the Maxwell equation

$$\nabla \times \mathbf{h}_s = \frac{4\pi}{c} \mathbf{j}_s. \quad (42)$$

Let us for a moment ignore complications arising from the screening effects and consider only the vector potential  $\mathbf{A}_0$ . This is permissible, since as it will become clear later, corrections to Eqs. (40) from the screening field are of the same higher order in the small parameter  $(H_{c2} - H)/H_{c2}$  as the nonlinear terms which have been neglected in these equations. In the same spirit as the original Abrikosov<sup>20</sup> treatment, these higher order terms will be included variationally in a later stage of the calculation.

It is easily seen that in the Landau gauge  $\mathbf{A}_0 = \hat{y}Hx$  the linearized field equations (40) are satisfied by taking

$$d(\mathbf{r}) = e^{iky}d(x), \quad s(\mathbf{r}) = e^{iky}s(x). \quad (43)$$

Thus, exactly as in the one component case first studied by Abrikosov,<sup>20</sup> we are left with a one dimensional problem which can be stated as follows:

$$\left\{ \alpha_d + \left[ \frac{p^2}{2m} + \frac{1}{2} m \omega_c^2 (x - x_k)^2 \right] \right\} d + \epsilon_v \left[ -\frac{p^2}{2m} + \frac{1}{2} m \omega_c^2 (x - x_k)^2 \right] s = 0, \quad (44a)$$

$$\epsilon_v \left[ -\frac{p^2}{2m} + \frac{1}{2} m \omega_c^2 (x - x_k)^2 \right] d + \left\{ \alpha_s + \left[ \frac{p^2}{2m} + \frac{1}{2} m \omega_c^2 (x - x_k)^2 \right] \right\} s = 0. \quad (44b)$$

Here we have denoted  $p = -i\hbar \partial / \partial x$ ,  $x_k = kl^2$ , and  $\omega_c = (e^* H / mc)$ . The magnetic length  $l = \sqrt{\hbar c / e^* H}$  will play the role of a characteristic length for the vortex lattice. We also assume henceforth that  $m_d^* = m_s^* \equiv m$ , i.e., that  $\gamma_d = \gamma_s$ , and we use  $\epsilon_v = \gamma_v / \gamma_s = m_s^* / m_v^*$ . Equations (44) resemble those for the quantum mechanical harmonic oscillator problem with the potential centered at  $x = x_k$ . In view of the fact that  $x_k$  is arbitrary, it is clear that Eqs. (44) will have infinitely many degenerate solutions which can be labeled by a continuous index  $k$ . This degeneracy will play a crucial role later when we construct the periodic space-filling solution. However, for the moment, we shall ignore this issue and investigate Eqs. (44) with  $x_k$  fixed. The essential difference from the one component case is that these equations have no obvious exact solutions. In what follows we shall seek suitable variational solutions to Eqs. (44). In order to stress the analogy with the harmonic oscillator, we may write (44) in the following way:

$$(\mathcal{H}_0 + \alpha_d)d + Vs = Ed, \quad (45a)$$

$$Vd + (\mathcal{H}_0 + \alpha_s)s = Es, \quad (45b)$$

where  $\mathcal{H}_0 = \hbar \omega_c (a^\dagger a + 1/2)$  and  $V = \epsilon_v (\hbar \omega_c / 2) (a^\dagger a^\dagger + aa)$  are expressed in terms of the usual raising and lowering operators, which can be written as  $a = [(x - x_k) / l + l(\partial / \partial x)] / \sqrt{2}$ . By including the right hand side of Eqs. (45) we are considering a slightly more general problem:  $E = 0$  corresponds to the physical solution for  $H = H_{c2}(T)$ , and solutions for  $E < 0$  will be useful later when we consider the stability of various vortex lattice structures.

In order to motivate our variational solution to the linearized problem, let us define

$$\mathcal{H}^\pm = \mathcal{H}_0 \pm V, \quad \varphi^\pm = d \pm s. \quad (46)$$

In terms of these variables, the set of equations (45) becomes

$$\begin{pmatrix} \mathcal{H}^+ + T - T^* & -\Delta T / 2 \\ -\Delta T / 2 & \mathcal{H}^- + T - T^* \end{pmatrix} \begin{pmatrix} \varphi^+ \\ \varphi^- \end{pmatrix} = E \begin{pmatrix} \varphi^+ \\ \varphi^- \end{pmatrix}, \quad (47)$$

where we have defined

$$T^* = (T_d + T_s) / 2, \quad \Delta T = T_d - T_s, \quad (48)$$

for convenience in later calculations. A nice feature of the representation (47) is that for the degenerate case  $\Delta T=0$  the equations for  $\varphi^+$  and  $\varphi^-$  decouple, each becoming a simple harmonic oscillator problem. Motivated by this fact we shall seek the variational solution for the general case in the form of normalized ground state wave-functions of the harmonic oscillator,

$$\varphi_k^\pm(x) = \sqrt{\frac{\sigma_\pm}{l\sqrt{\pi}}} e^{-\sigma_\pm^2(x-x_k)^2/2l^2}. \quad (49)$$

The variational parameters  $\sigma_+$  and  $\sigma_-$  will be determined by minimization of the eigenvalue<sup>32</sup>

$$\begin{aligned} \langle E \rangle &= (T - T^*) + \frac{1}{2} \langle \varphi^+ | \mathcal{H}^+ | \varphi^+ \rangle + \frac{1}{2} \langle \varphi^- | \mathcal{H}^- | \varphi^- \rangle \\ &\quad - \frac{1}{2} \Delta T \langle \varphi^+ \varphi^- \rangle, \end{aligned} \quad (50)$$

where angular brackets stand for spatial averages. All the integrals are easily evaluated and if one defines  $\sigma_+ = \sigma \cos \vartheta$ ,  $\sigma_- = \sigma \sin \vartheta$ , the resulting expression for  $\langle E \rangle$  can be explicitly minimized with respect to  $\sigma^2$ . The minimum occurs for  $\sigma^2 = \tan \vartheta + 1/\tan \vartheta$ , and is

$$\begin{aligned} \frac{\langle E \rangle}{\Delta T} &= \frac{T - T^*}{\Delta T} + \frac{1}{4} \left( \frac{\hbar \omega_c}{\Delta T} \right) \left[ (1 + \epsilon_v) \tan \vartheta + (1 - \epsilon_v) \frac{1}{\tan \vartheta} \right] \\ &\quad - \frac{1}{2} \sqrt{\frac{2 \tan \vartheta}{1 + \tan^2 \vartheta}}. \end{aligned} \quad (51)$$

The last equation must be minimized numerically with respect to  $\tan \vartheta$ . It is also clear from this equation that two parameters,  $\epsilon_v$  and

$$\Lambda = \hbar \omega_c / \Delta T, \quad (52)$$

determine the nature of the variational solution. In the two limiting cases the exact minimum can be easily found. In the low field limit,  $\Lambda \ll 1$ , we have  $\sigma_+ \approx \sigma_- \approx 1$ , while in the high field limit,  $\Lambda \gg 1$ , we have  $\sigma_\pm \approx [(1 \pm \epsilon_v)/(1 \mp \epsilon_v)]^{1/4}$ . It follows that at least intermediate values of  $\Lambda$  are required for appreciable effects from  $s$ - $d$  mixing to occur. Otherwise  $\varphi^+ \approx \varphi^-$  and according to Eq. (46) the  $s$  component effectively vanishes.

Solutions to Eq. (51) with  $\langle E \rangle = 0$  give the dependence of the upper critical field  $H_{c2}$  on the temperature. Whenever a finite admixture of the  $s$  component is present, we find a characteristic upward curvature in  $H_{c2}(T)$  near the critical temperature. Such curvature has been observed experimentally in both La-Sr-Cu-O (LSCO) and YBCO compounds<sup>33,34</sup> and has been interpreted as a consequence of  $s$ - $d$  mixing.<sup>12,14</sup> For given parameters  $T_d$  and  $T_s$  and several values of  $\epsilon_v$  such dependence is shown in Fig. 9, as obtained by numerical minimization of Eq. (51).

### B. Vortex lattice solution

To construct a periodic vortex lattice, consider a linear superposition of the basis functions (49) of the form

$$\Psi_\pm(\mathbf{r}) = \sum_n c_n e^{in_q y} \varphi_n^\pm(x), \quad (53)$$

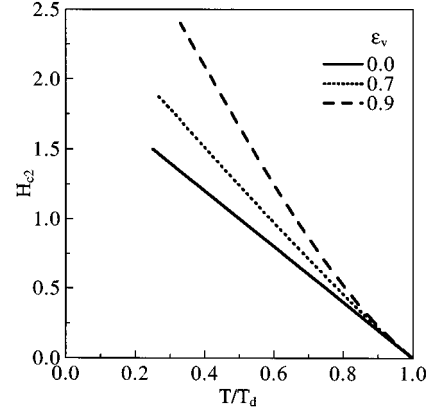


FIG. 9. Dependence of upper critical field  $H_{c2}(T)$  on temperature for various values of parameter  $\epsilon_v$  and  $T_s = 0.5T_d$ ,  $T = 0.75T_d$ .

where  $c_n$  are complex constants. In order to impose periodicity in  $y$  direction we have constrained the values of  $k$  to integer multiples

$$k_n = nq, \quad n = 0, \pm 1, \pm 2, \dots \quad (54)$$

of the parameter  $q$  which will be determined later from the requirement of minimum free energy. The space filling solutions of GL equations can be written as, cf. Eq. (46),

$$d(\mathbf{r}) = [\Psi_+(\mathbf{r}) + \Psi_-(\mathbf{r})]/2,$$

$$s(\mathbf{r}) = [\Psi_+(\mathbf{r}) - \Psi_-(\mathbf{r})]/2. \quad (55)$$

These solutions will also be periodic in  $x$  provided that the constants  $c_n$  satisfy the condition  $c_{n+N} = c_n$  for some integer  $N$ . As was first noted by Abrikosov,<sup>20</sup> the analysis of the vortex lattice for general  $N$  is extremely difficult. It was however conjectured that the absolute minimum of the free energy takes place for  $N \leq 2$ , in which case the analysis is simplified. In what follows we shall restrict ourselves to the case of  $N=2$  for the two component system. Taking  $N=2$  we have  $c_{2n} = c_0$  and  $c_{2n+1} = c_1$ . This, along with Eqs. (54) and (55), implies periodicity of  $s$  and  $d$  in  $x$  and  $y$  with periods

$$L_x = 2l^2q, \quad L_y = 2\pi/q. \quad (56)$$

Each rectangular  $L_x \times L_y$  unit cell then contains an amount of flux

$$HL_x L_y = 2(hc/e^*) \equiv 2\Phi_0, \quad (57)$$

where  $\Phi_0$  stands for the flux quantum. Thus, by construction, each rectangular unit cell contains exactly two singly quantized vortices, independent of the value of parameter  $q$ . The resulting vortex lattice may be thought of as centered rectangular with two quanta per unit cell or, equivalently, as an oblique cell with lattice vectors of equal length and one flux quantum. While the restriction to centered rectangular lattices is made primarily for computational convenience, it is also compatible with recent experiments on YBCO which show evidence<sup>22,23</sup> for oblique vortex lattices with nearly equal lattice constants in high fields.

The parameter  $q$  controls the shape of the unit cell. It is customary to define the ratio

$$R = L_x/L_y = (l^2/\pi)q^2, \quad (58)$$

and it follows that  $R=1$  corresponds to the square,  $R=\sqrt{3}$  corresponds to the triangular, and intermediate values  $1 < R < \sqrt{3}$  imply the oblique vortex lattice.

The solution that we have constructed for the GL equations (8) has three free parameters,  $c_0$ ,  $c_1$ , and  $R$ . These parameters determine the structure of the vortex lattice near  $H_{c2}$ . Within the linearized approximation to the GL free energy these solutions are degenerate in energy. It is the fourth order terms that lift this degeneracy and determine the equilibrium lattice structure. In order to find this minimum one must take into account the fourth order terms in the free energy (1) as well as the effects of screening which were so far ignored.

The complete average free energy density (1) can be written as

$$\langle f \rangle = \langle f_2 \rangle + \langle f_4 \rangle + \langle h^2 \rangle / 8\pi, \quad (59)$$

where  $f_2$  and  $f_4$  stand for quadratic and quartic invariants respectively, and  $\mathbf{h} = \mathbf{H} + \mathbf{h}_s$  is the local magnetic field. Let us now consider the effect of screening by looking at the gradient terms in  $\langle f_2 \rangle$  with the complete  $\vec{\Pi}$  as given by Eq. (41). A typical term will be of the form

$$\begin{aligned} \langle |\vec{\Pi}d|^2 \rangle &= \langle |\vec{\Pi}_0d + \vec{\Pi}_s d|^2 \rangle \approx \langle |\vec{\Pi}_0d|^2 \rangle + \langle \vec{\Pi}_s \cdot [d^* \vec{\Pi}_0 d \\ &+ \text{c.c.}] \rangle, \end{aligned} \quad (60)$$

where in the last equality terms of the order of  $|\vec{\Pi}_s d|^2$  have been neglected. This is consistent with the general idea of GL theory of keeping only terms up to fourth order in the order parameters. Being proportional to the supercurrent,  $\vec{\Pi}_s$  already contains terms quadratic in the order parameters. If we expand all the remaining gradient terms in the similar way, systematically neglecting terms containing order parameters to powers higher than 4, we can write the result as

$$\langle f_2 \rangle = \langle f_2^{(0)} \rangle + \frac{\hbar}{e^*} \langle \vec{\Pi}_s \cdot \mathbf{j}_s \rangle. \quad (61)$$

Here  $f_2^{(0)}$  is the part of  $f_2$  containing only the  $\vec{\Pi}_0$  piece of the gauge invariant gradient, i.e., the quadratic part in the absence of screening, and similarly  $\mathbf{j}_s$  is assumed to be given by Eq. (9) with  $\vec{\Pi} = \vec{\Pi}_0$ . If we take into account the property of the variational solution  $\langle f_2^{(0)} \rangle = E \langle |s|^2 + |d|^2 \rangle$  that follows from Eqs. (45) and use the definition of  $\vec{\Pi}_s$  we can write

$$\langle f \rangle = E \langle |s|^2 + |d|^2 \rangle - (1/c) \langle \mathbf{A}_s \cdot \mathbf{j}_s \rangle + \langle f_4 \rangle + \langle (\mathbf{H} + \mathbf{h}_s)^2 \rangle / 8\pi, \quad (62)$$

The second term on the right-hand side (RHS) can be simplified by expressing  $\mathbf{j}_s$  through the Maxwell equation (42). Integrating by parts and neglecting the surface term one obtains  $(1/c) \langle \mathbf{A}_s \cdot \mathbf{j}_s \rangle = \langle h_s^2 \rangle / 4\pi$ .

Similarly the last term on the RHS can be rewritten recalling the definition  $\mathbf{B} = \mathbf{H} + \langle \mathbf{h}_s \rangle$  of the magnetic induction as  $\langle h_s^2 \rangle / 8\pi - H^2 / 8\pi + \mathbf{B} \cdot \mathbf{H} / 4\pi$ .

The manipulations performed above are useful since in fixed applied magnetic field the proper thermodynamic potential to minimize is the mean Gibbs free energy density related to  $f$  by  $\langle g \rangle = \langle f \rangle - \mathbf{B} \cdot \mathbf{H} / 4\pi$ . For this quantity we finally arrive at an expression

$$\langle g \rangle = E \langle |s|^2 + |d|^2 \rangle + \langle f_4 \rangle - \langle h_s^2 \rangle / 8\pi - H^2 / 8\pi. \quad (63)$$

Before we proceed with minimization of the Gibbs potential let us notice that the simple thermodynamic relation  $\partial \langle g \rangle / \partial H = -B / 4\pi$  can be used to extract the average screening field in the superconductor

$$\langle h_s \rangle = B - H = - \left( \frac{\partial E}{\partial H} \right) \langle |s|^2 + |d|^2 \rangle. \quad (64)$$

A similar relation between the average induced field and the order parameter for the conventional  $s$ -wave superconductor<sup>20</sup> is known as the ‘‘first Abrikosov identity,’’ but the corresponding determination of the spatial distribution of  $\mathbf{h}_s(\mathbf{r})$  is more complicated (see below). It is easy to verify that in the limit  $\epsilon_v \rightarrow 0$  (i.e., in the limit of pure  $d$  wave) Eq. (64) assumes the precise form of this identity, including all the relevant prefactors that follow upon expressing  $\partial E / \partial H$  from Eq. (51). In the vicinity of  $H_{c2}$  it holds that  $E \approx (\partial E / \partial H)(H - H_{c2})$  and it follows that to the leading order we can write  $\langle f_2^{(0)} \rangle = \langle h_s \rangle (H_{c2} - H) / 4\pi$ . This allows us to express the Gibbs free energy in the form where the leading dependence on the magnetic field  $H$  is manifestly displayed:

$$\langle g \rangle - \langle g \rangle_n = \frac{1}{4\pi} (H_{c2} - H) \langle h_s \rangle + \langle f_4 \rangle - \frac{1}{8\pi} \langle h_s^2 \rangle, \quad (65)$$

with  $\langle g \rangle_n = -H^2 / 8\pi$  being the normal state contribution to the Gibbs free energy.

Consider now a simple scaling transformation  $(s, d) \rightarrow (\lambda s, \lambda d)$  where  $\lambda$  is a real number. It is clear that under such a transformation  $\langle h_s \rangle \rightarrow \lambda^2 \langle h_s \rangle$ , while  $\langle f_4 \rangle \rightarrow \lambda^4 \langle f_4 \rangle$  and  $\langle h_s^2 \rangle \rightarrow \lambda^4 \langle h_s^2 \rangle$ . Consequently, the Gibbs free energy (65) will have a well defined minimum for the particular value of  $\lambda$ . We use this property to determine the normalization of the order parameters  $s$  and  $d$ . Carrying out the minimization we obtain

$$\langle g \rangle - \langle g \rangle_n = - \frac{1}{8\pi} \frac{(H_{c2} - H)^2 \langle h_s \rangle^2}{8\pi \langle f_4 \rangle - \langle h_s^2 \rangle}, \quad (66)$$

an expression which is clearly independent of the particular normalization of  $s$  and  $d$ . If we further define the Abrikosov ratio  $\beta_A$  and the Ginzburg-Landau parameter  $\kappa$  by

$$\beta_A = \frac{\langle h_s^2 \rangle}{\langle h_s \rangle^2}, \quad \kappa^2 = 4\pi \frac{\langle f_4 \rangle}{\langle h_s^2 \rangle}, \quad (67)$$

we can write the resulting Gibbs free energy for the Abrikosov vortex lattice in the familiar form<sup>20</sup>

$$\langle g \rangle - \langle g \rangle_n = - \frac{1}{8\pi} \frac{(H_{c2} - H)^2}{(2\kappa^2 - 1)\beta_A}. \quad (68)$$

Several remarks are in order. The Abrikosov ratio  $\beta_A$  defined by Eq. (67) is independent of the coefficients  $\beta_i$  in the quar-

tic part of the free energy and depends only on the shape of the unit cell in the vortex lattice. To the extent that  $\kappa$  is independent of the specific lattice shape, the minimum Gibbs free energy corresponds to the minimum of  $\beta_A$ , which generalizes the familiar Abrikosov result, apart from writing it in terms of magnetic field instead of the absolute squared order parameter. As will be shown below by numerical calculation, it is indeed true that the parameter  $\kappa$  defined by Eq. (67) depends only very weakly on the vortex lattice shape, and thus the factor  $(2\kappa^2 - 1)$  in the denominator of Eq. (68) serves simply as the criterion for type-II behavior, which occurs only for  $\kappa > 1/\sqrt{2}$ . It is in this sense that one can think of  $\kappa$  as a generalization of the conventional Ginzburg-Landau parameter; we note that  $\kappa$  defined by Eq. (67) cannot be simply related to the usual ratio of penetration depth  $\lambda$  to coherence length  $\xi$ . This difficulty is related to the fact that in the presence of two order parameters  $s$  and  $d$  we have, strictly speaking, two distinct coherence lengths,  $\xi_s$  and  $\xi_d$ . Most observable phenomena will only reveal a single "effective" coherence length given by a certain combination of  $\xi_s$  and  $\xi_d$ , but this will presumably depend on the type of probe used in the experiment. By contrast, there will be only single penetration depth  $\lambda$ , as this quantity is related to the decay of the magnetic field inside the superconductor. Alternatively,  $\lambda$  may be viewed as a measure of the bulk superfluid density, which is in the present case associated with the  $d$ -wave component only, since the  $s$  wave vanishes in the bulk. Thus it may be suggested that  $\kappa = \lambda/\xi_A$ , where  $\xi_A$  is the effective coherence length relevant to the Abrikosov lattice, determined by the usual criterion of overlapping vortex cores at  $H = H_{c2}$ .

### C. Magnetic field distribution

The ultimate goal of this section is to determine the actual structure of the vortex lattice by minimizing the Gibbs free energy given by Eq. (68). To obtain the parameters  $\beta_A$  and  $\kappa$  that enter this expression it will be necessary to evaluate the spatial averages  $\langle f_4 \rangle$  and  $\langle h_s^2 \rangle$  [note that the quantity  $\langle h_s \rangle$  has been already calculated in Eq. (64) by a thermodynamic argument]. The former of the two averages can be computed in a fairly straightforward manner since  $f_4$  is directly related to the vortex lattice solutions  $\Psi_{\pm}(\mathbf{r})$ , which are simple linear superpositions of the Gaussian wave functions  $\varphi_k^{\pm}$  given by Eq. (49). The situation with the other average,  $\langle h_s^2 \rangle$ , is more complicated as one has to first invert the Maxwell equation (42) in order to express the local screening field  $\mathbf{h}_s(\mathbf{r})$  in terms of the supercurrent  $\mathbf{j}_s$ . Both of these quantities are themselves of interest, as they can be measured in principle by various experimental probes (see Sec. V for the discussion).

With this in mind let us calculate the spatial distribution of the screening field. If we express  $\mathbf{h}_s$  in terms of the vector potential  $\mathbf{A}_s$ , the Maxwell equation (42) can be written as

$$\nabla^2 \mathbf{A}_s = -\frac{4\pi}{c} \mathbf{j}_s, \quad (69)$$

where we have taken advantage of the fact that the Landau gauge satisfies  $\nabla \cdot \mathbf{A}_s = 0$ . The easiest way to invert Eq. (69)

is to exploit the periodicity of the vortex lattice solution and work in Fourier space. If we write

$$\mathbf{j}_s(\mathbf{r}) = \sum_{\mathbf{k}} e^{i\mathbf{k} \cdot \mathbf{r}} \mathbf{j}_s(\mathbf{k}), \quad \mathbf{A}_s(\mathbf{r}) = \sum_{\mathbf{k}} e^{i\mathbf{k} \cdot \mathbf{r}} \mathbf{A}_s(\mathbf{k}), \quad (70)$$

where the summation goes over the reciprocal lattice vectors  $\mathbf{k} = (k_x, k_y) \equiv (2\pi k_1/L_x, 2\pi k_2/L_y)$  and  $(k_1, k_2) = 0, \pm 1, \pm 2, \dots$ , Eq. (69) implies that

$$\mathbf{A}_s(\mathbf{k}) = \frac{4\pi}{c} \frac{\mathbf{j}_s(\mathbf{k})}{k^2}, \quad \mathbf{k} \neq 0. \quad (71)$$

Thus, one obtains for the Fourier components of the screening field,

$$\mathbf{h}_s(\mathbf{k}) = \frac{4\pi i}{c} \frac{\mathbf{k} \times \mathbf{j}_s(\mathbf{k})}{k^2}, \quad \mathbf{k} \neq 0. \quad (72)$$

In order to evaluate this expression it is helpful to write the supercurrent (9) using wavefunctions  $\Psi_{\pm}$  instead of  $s$  and  $d$ :

$$\begin{aligned} \mathbf{j}_s(\mathbf{r}) = & \delta \frac{e^* \hbar}{4m} \sum_{\alpha=\pm} [\hat{x}(1 - \alpha \epsilon_v) \Psi_{\alpha}^* \Pi_x \Psi_{\alpha} \\ & + \hat{y}(1 + \alpha \epsilon_v) \Psi_{\alpha}^* \Pi_y \Psi_{\alpha} + \text{c.c.}]. \end{aligned} \quad (73)$$

In order to model the layered structure of cuprate superconductors we have introduced the usual geometrical factor  $\delta = (\text{layer thickness}/\text{layer spacing})$ . The case  $\delta = 1$  corresponds to the cubic lattice, while  $\delta \rightarrow 0$  represents the limit of a single isolated layer. In this notation, the Fourier components of the supercurrent are

$$\begin{aligned} \mathbf{j}_s(\mathbf{k}) = & \delta \frac{e^* \hbar}{4m} \sum_{\alpha=\pm} [\hat{x}(1 - \alpha \epsilon_v) \langle \Psi_{\alpha}^* \Pi_x \Psi_{\alpha} \rangle_{\mathbf{k}} \\ & + \hat{y}(1 + \alpha \epsilon_v) \langle \Psi_{\alpha}^* \Pi_y \Psi_{\alpha} \rangle_{\mathbf{k}} + \langle \text{c.c.} \rangle_{-\mathbf{k}}]. \end{aligned} \quad (74)$$

Here we have introduced a shorthand notation

$$\langle \dots \rangle_{\mathbf{k}} \equiv \frac{1}{L_x L_y} \int_0^{L_x} dx \int_0^{L_y} dy \dots e^{-i\mathbf{k} \cdot \mathbf{r}}, \quad (75)$$

which will prove very convenient in the subsequent calculations. With some effort, the following useful relations can be derived:

$$\begin{aligned} \langle \Psi_{\alpha}^* \Pi_x \Psi_{\alpha} \rangle_{\mathbf{k}} &= \frac{\sigma_{\alpha}}{2} \left( \frac{k_x}{\sigma_{\alpha}} - ik_y \sigma_{\alpha} \right) \langle |\Psi_{\alpha}|^2 \rangle_{\mathbf{k}}, \\ \langle \Psi_{\alpha}^* \Pi_y \Psi_{\alpha} \rangle_{\mathbf{k}} &= \frac{i}{2\sigma_{\alpha}} \left( \frac{k_x}{\sigma_{\alpha}} - ik_y \sigma_{\alpha} \right) \langle |\Psi_{\alpha}|^2 \rangle_{\mathbf{k}}. \end{aligned} \quad (76)$$

In real space,  $\Psi_{\alpha}(\mathbf{r})$  is a linear combination of Gaussians, and thus the Fourier components  $\langle |\Psi_{\alpha}|^2 \rangle_{\mathbf{k}}$  are easily evaluated. One obtains

$$\langle |\Psi_\alpha|^2 \rangle_{\mathbf{k}} = \frac{a_{\mathbf{k}}}{L_x} \exp \left\{ -\frac{l^2}{4} [(k_x/\sigma_\alpha)^2 + (k_y\sigma_\alpha)^2] \right\}, \quad (77)$$

where

$$a_{\mathbf{k}} = e^{i\frac{\pi}{2}k_1k_2} [c_0c_{k_2}^* + (-1)^{k_1}c_1c_{k_2+1}^*] \quad (78)$$

are real constants, independent of the particular lattice shape. Substituting relations (76) in the expression for the supercurrent (74) one obtains

$$\begin{aligned} \mathbf{j}_s(\mathbf{k}) = & i\delta \frac{e^*\hbar}{4m} \sum_{\alpha=\pm} [\hat{x}(1-\alpha\epsilon_v)(-k_y\sigma_\alpha^2) \\ & + \hat{y}(1+\alpha\epsilon_v)(k_x/\sigma_\alpha^2)] \langle |\Psi_\alpha|^2 \rangle_{\mathbf{k}}. \end{aligned} \quad (79)$$

This expression is particularly useful for numerical evaluation of the real space supercurrent distribution, since in view of the Gaussian dependence of  $\langle |\Psi_\alpha|^2 \rangle_{\mathbf{k}}$  on  $\mathbf{k}$  [cf. Eq. (77)] it is clear that the corresponding Fourier series will converge very rapidly.

Finally, we are in the position to give the local screening field. Substitution of the above equation (79) into the Maxwell equation (72) yields all the Fourier components of the field with  $\mathbf{k} \neq 0$ . The  $\mathbf{k}=0$  component is just the real space average of the screening field  $\langle h_s \rangle$  given by Eq. (64). Combining these results we obtain, after some algebra, the real space field distribution of the form

$$\begin{aligned} \mathbf{h}_s(\mathbf{r}) = & -\hat{z}\pi\delta \frac{e^*\hbar}{mc} \left[ z_0 \sum_{\mathbf{k}} e^{i\mathbf{k}\cdot\mathbf{r}} \langle |\Psi_+|^2 + |\Psi_-|^2 \rangle_{\mathbf{k}} \right. \\ & \left. + z_1 \sum_{\mathbf{k} \neq 0} e^{i\mathbf{k}\cdot\mathbf{r}} \left( \frac{k_x^2 - k_y^2}{k_x^2 + k_y^2} \right) \langle |\Psi_+|^2 - |\Psi_-|^2 \rangle_{\mathbf{k}} \right], \end{aligned} \quad (80)$$

where we have defined the numerical factors

$$\begin{aligned} z_0 = & [(\sigma_-^2 + \sigma_+^2) + \epsilon_v(\sigma_-^2 - \sigma_+^2)]/2, \\ z_1 = & [(\sigma_-^2 - \sigma_+^2) + \epsilon_v(\sigma_-^2 + \sigma_+^2)]/2. \end{aligned} \quad (81)$$

We notice that the first Fourier sum in the brackets of Eq. (80) is equal to  $|\Psi_+(\mathbf{r})|^2 + |\Psi_-(\mathbf{r})|^2 \equiv 2(|s(\mathbf{r})|^2 + |d(\mathbf{r})|^2)$ . Thus in the limit of a pure  $d$ -wave state where  $\epsilon_v \rightarrow 0$  and  $\sigma_\pm \rightarrow 1$  the correspondence with the Abrikosov result for a conventional superconductor becomes transparent. In this limit we have  $z_0 \rightarrow 1$ ,  $z_1 \rightarrow 0$  and  $|s(\mathbf{r})| \rightarrow 0$ , and the spatially varying form of the Abrikosov first identity is recovered, with  $d(\mathbf{r})$  playing the role of the conventional order parameter  $\Psi(\mathbf{r})$ . The second sum clearly has a nonlocal dependence on the order parameters and can be written as  $\int d^2r' g(\mathbf{r}-\mathbf{r}') [s(\mathbf{r}')d^*(\mathbf{r}') + s^*(\mathbf{r}')d(\mathbf{r}')]$ . Such a term has no counterpart in the conventional theory, and arises only

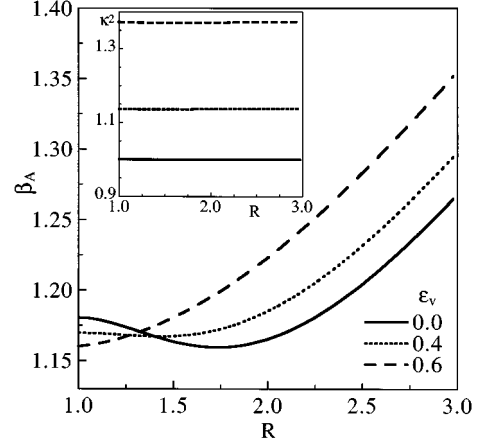


FIG. 10. Abrikosov ratio  $\beta_A$  as a function of the lattice geometry factor  $R=L_x/L_y$  for different values of  $\epsilon_v$ . Note that the minimum of  $\beta_A$  is moving from  $R=\sqrt{3}$  to  $R=1$  as  $\epsilon_v$  increases. This implies a continuous deformation of the initially triangular vortex lattice into an oblique and finally square lattice. The parameters used are  $T_s=0.5T_d$ ,  $T=0.75T_d$ ,  $\beta_1=\beta_2=\beta_3=\beta_4=1$ , and  $B=0.8H_{c2}$ . The inset shows the  $R$  dependence of the squared Ginzburg-Landau ratio  $\kappa^2$  on approximately the same scale.

as a result of mixing between the  $s$  and  $d$  components of the order parameter. The nonlocality of this term is a direct consequence of the symmetry of the problem: since by itself the term  $(sd^* + s^*d)$  is not invariant under  $D_4$ , it can enter only in combination with other terms of proper symmetry.

#### D. Structure of the vortex lattice

As mentioned above, in order to determine the shape of the vortex lattice, one needs to evaluate the averages of the fourth order terms  $\langle f_4 \rangle$  and  $\langle h_s^2 \rangle$ . Now that the distribution of the magnetic field  $\mathbf{h}(\mathbf{r})$  has been derived, evaluation of these averages is a straightforward, albeit quite a lengthy, procedure. The technical details of this calculation are worked out in the Appendix, and here we only summarize the results and discuss some of the physical implications.

Equations (94) and (99) of the Appendix give the expressions for the fourth order averages  $\langle f_4 \rangle$  and  $\langle h_s^2 \rangle$  in terms of rapidly converging sums that are suitable for numerical evaluation. Making use of these, the Abrikosov ratio and Ginzburg-Landau parameter can be expressed in the following simple way:

$$\beta_A = \frac{L_x^2}{4z_0^2} \sum_{\mathbf{k}} ' [(z_0 + z_1 \eta_{\mathbf{k}}) \Omega_{++}(\mathbf{k}) + (z_0 - z_1 \eta_{\mathbf{k}}) \Omega_{--}(\mathbf{k})]^2, \quad (82)$$

and

$$\kappa^2 = \frac{4 \sum_{\mathbf{k}} ' \sum_{\alpha} [\mu_1 \Omega_{\alpha\alpha}^2(\mathbf{k}) + \mu_2 \Omega_{\alpha\alpha}(\mathbf{k}) \Omega_{\bar{\alpha}\bar{\alpha}}(\mathbf{k}) + \mu_3 \Omega_{\alpha\alpha}(\mathbf{k}) \Omega_{\alpha\bar{\alpha}}(\mathbf{k}) + \mu_4 \Omega_{\alpha\bar{\alpha}}^2(\mathbf{k})]}{\pi \delta^2 (e^*\hbar/mc)^2 \sum_{\mathbf{k}} ' [(z_0 + z_1 \eta_{\mathbf{k}}) \Omega_{++}(\mathbf{k}) + (z_0 - z_1 \eta_{\mathbf{k}}) \Omega_{--}(\mathbf{k})]^2}, \quad (83)$$

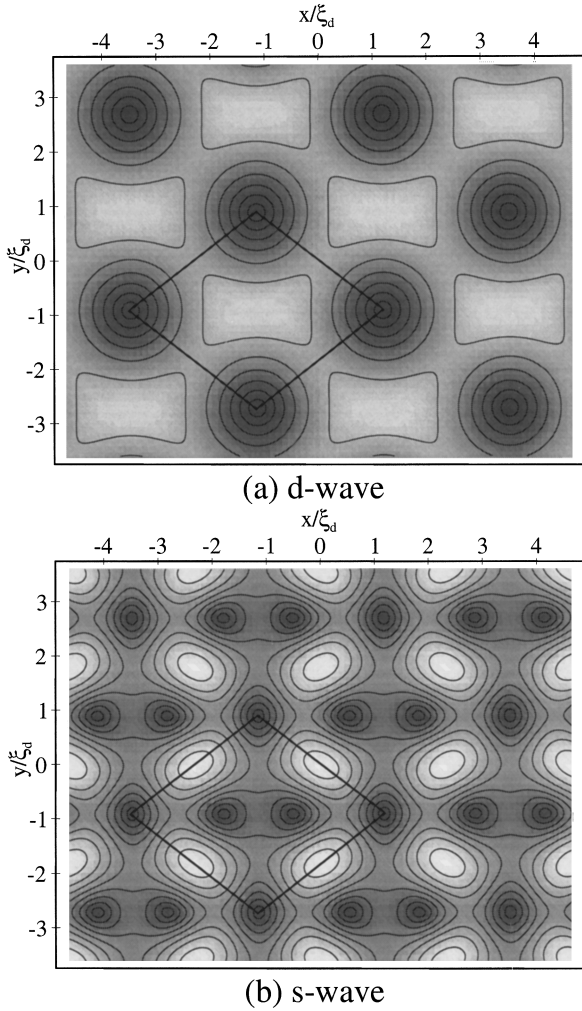


FIG. 11. Contour plot of the amplitudes of (a)  $d$  component and (b)  $s$  component of the order parameter in the vortex lattice. The same parameters are used as in Fig. 10 with  $\epsilon_v = 0.45$  resulting in an oblique vortex lattice with  $R_{\min} = 1.29$  and the angle between primitive vectors  $\phi = 76^\circ$ . The oblique unit cell containing one flux quantum is marked by a solid line.

where the prime on the sums means that only terms with  $k_1$  and  $k_2$  both even or odd are included,  $\Omega_{\alpha\beta}(\mathbf{k})$  are Gaussian functions given explicitly by Eq. (93),  $\eta_{\mathbf{k}}$  is a simple function defined by Eq. (97), and  $\bar{\alpha} = -\alpha$ . Note that the above expression for  $\beta_A$  is independent of parameters  $\beta_i$  that enter the quartic part of the free energy  $f_4$ , and other quadratic parameters enter only via the variational parameters  $\sigma_{\pm}$ .

The shape of the vortex lattice unit cell is determined by the ratio  $R = L_x/L_y$ . The value of  $R$  that corresponds to the thermodynamically stable configuration,  $R_{\min}$ , is obtained by requiring that the Gibbs free energy is minimum. Equation (68) shows that, at given external magnetic field  $H$ , the Gibbs free energy  $\langle g \rangle$  is entirely determined by the two parameters given above,  $\beta_A$  and  $\kappa$ . Numerical evaluation of these parameters confirms that  $\kappa$  is only very weakly dependent on the particular lattice shape, as it is illustrated by Fig. 10. The dependence of the Gibbs free energy (68) on  $R$  is almost entirely contained in the Abrikosov ratio  $\beta_A$  and thus, in most of the parameter space, the minimum of  $\langle g \rangle$  coin-

cides to a good accuracy with the minimum of  $\beta_A$ . For example in the particular case displayed in Fig. 10, the minimum of  $\beta_A$  differs by less than 2% from the minimum the full free energy.

Figure 10 also shows a typical dependence of  $\beta_A$  on  $R$  for different values of the mixed gradient coupling  $\epsilon_v$ , as obtained by numerical evaluation of Eq. (82). When  $\epsilon_v = 0$  the superconductor is in a pure  $d$ -wave state with no  $s$ -wave component present. Within the phenomenological GL theory, this situation is identical to the case of a conventional superconductor studied by Abrikosov. Thus, the state with minimum free energy has  $R_{\min} = \sqrt{3}$  which corresponds to the usual triangular vortex lattice. In this limit we obtain the correct value of  $\beta_A = 1.1596$  as quoted by Kleiner *et al.*<sup>21</sup> However, as soon as a nonzero coupling  $\epsilon_v$  is introduced, the situation changes and the minimum of  $\beta_A$  shifts to the values  $R_{\min} < \sqrt{3}$ , signalling that an oblique vortex lattice is favored. The minimum  $R_{\min}$  varies continuously with  $\epsilon_v$  and at certain value of  $\epsilon_v$ , which depends on the other parameters in the GL free energy,  $R_{\min}$  reaches the value of 1, corresponding to the square lattice. Further increase of  $\epsilon_v$  then has no effect on the shape of the lattice, which remains square.

One may conclude that in a  $d$ -wave superconductor, in the regime close to the upper critical field  $H_{c2}$ , a general oblique vortex lattice is thermodynamically stable, unless the material is in one of the limiting regimes in which the mixed gradient coupling  $\epsilon_v$  is very small or very large. Numerical<sup>11</sup> and analytical<sup>15</sup> calculations based on the simple mean field model with proper symmetries, find evidence for a mixed gradient term of about the same order of magnitude as the conventional gradient terms. This would seem to argue against the two limiting cases mentioned above.

An example of the oblique vortex lattice is displayed in Fig. 11, where we show the  $d$  and  $s$  components of the order parameter as obtained by numerical evaluation of Eqs. (55), for a given set of GL parameters. An interesting conclusion can be drawn by comparing the two components of the order parameter: it is evident that the nontrivial nodal structure of the  $s$ -wave component, such as was described in Sec. III for an isolated vortex, persists in this high field regime. Indeed, zeros of  $s$  are present in the regions where  $|d| > 0$ . This quite remarkable result appears to suggest that the ‘‘extra’’ vortices in the  $s$  component are present over the entire portion of the phase diagram representing the mixed state of a  $d$ -wave superconductor.

Many experimental probes are sensitive to the spatial variations of the magnetic field rather than to the order parameter itself. The spatially varying component of the magnetic field,  $h_s(\mathbf{r})$ , as evaluated from Eq. (80) is shown in Fig. 12. Notice that as a consequence of the Maxwell equation  $\nabla \times \mathbf{h}_s = (4\pi/c)\mathbf{j}_s$ , it follows that the contours of constant magnetic field coincide with the supercurrent streamlines. Comparison to the order parameter plot in Fig. 11 confirms that the magnetic field and supercurrent distributions have the same symmetry as the vortex lattice. A nontrivial nodal structure of the  $s$  wave has an effect on the field distribution, which develops two nonequivalent saddle points, marked  $S1$  and  $S2$  in Fig. 12. In principle, it might be possible to determine such structure by  $\mu$ SR or NMR experiments. Figure 13

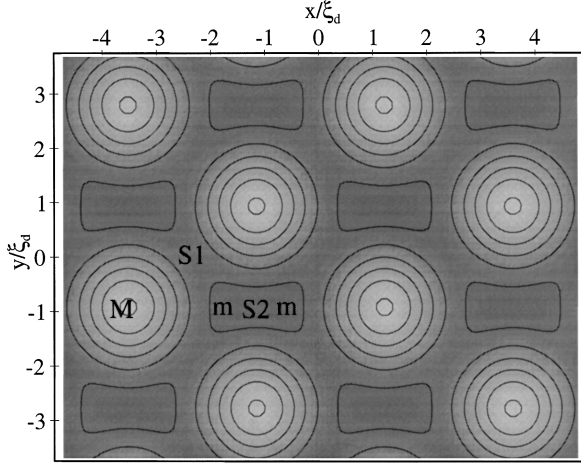


FIG. 12. Distribution of the magnetic field  $h_s$  in the vortex lattice. Letters  $M$ ,  $m$ ,  $S1$ , and  $S2$  denote the maximum, minimum, and two saddle points, respectively. GL parameters used for the plot are same as in Fig. 11.

displays the  $\mu$ SR line shapes that result from the magnetic field distribution as discussed above. The quantity shown is

$$P(h) = \frac{1}{L_x L_y} \int \delta[h - h(\mathbf{r})] d^2r, \quad (84)$$

for the case of triangular, oblique, and square flux lattices. In the triangular and square lattices, symmetry requires only one type of saddle point, resulting in the conventional single peak structure. In the oblique lattice, which is characteristic of a  $d$ -wave superconductor, the two nonequivalent saddle points give rise to two distinct Van Hove type singularities. Appearance of two distinct peaks in  $\mu$ SR or NMR spectra would provide evidence for  $d$ -wave behavior, since the explanations of oblique vortex lattice that invoke anisotropy within a single component model<sup>35</sup> do not lead to this effect.

### E. Orientation of the vortex lattice

The last subject that we want to address here concerns the spatial orientation of the vortex lattice with respect to the crystalline axes of the superconductor. From Fig. 11, it can be seen that the principal axes of the vortex lattice are not aligned with any of the high symmetry directions of the underlying crystal. Instead, it is the (110) direction of the vortex lattice that coincides with the (100) or (010) directions of the crystal. It turns out that the construction of the vortex lattice as presented above forces this particular orientation and does not allow for identical configurations that are rotated by some angle  $\alpha$ . In the traditional one component case, this is not a concern since the free energy has full rotational invariance. In the present case, however, we must take a closer look at these rotated configurations as we have terms in the free energy that break rotational invariance. It is conceivable that such rotated configurations might in fact be lower in free energy than the ones we have considered so far. In what follows we show by an explicit calculation that this

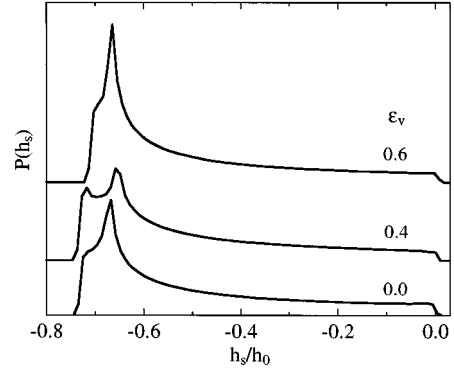


FIG. 13. Typical  $\mu$ SR line shapes as obtained from the magnetic field distribution in the vortex lattice. The curves shown are for triangular ( $\epsilon_v = 0.0$ ), oblique ( $\epsilon_v = 0.4$ ), and square ( $\epsilon_v = 0.6$ ) flux lattices. Magnetic field on the horizontal axis is in the units of  $h_0 = |\langle h_s \rangle| = 4\pi\delta(z_0/L_x)(e^*\hbar/mc)$  and the curves are offset vertically for clarity.

is not the case, and that we have in fact found the solution that corresponds to the absolute minimum of  $f$  as given by Eq. (1).

Consider a simple rotation of the coordinate system in the  $xy$  plane by an angle  $\alpha$

$$\begin{aligned} x &= x' \cos \alpha - y' \sin \alpha, \\ y &= x' \sin \alpha + y' \cos \alpha. \end{aligned} \quad (85)$$

Under such transformation all the second order terms are invariant except for the mixed gradient term which transforms as follows:

$$\begin{aligned} \frac{\partial s}{\partial y} \frac{\partial d^*}{\partial y} - \frac{\partial s}{\partial x} \frac{\partial d^*}{\partial x} + \text{c.c.} \\ = (\cos^2 \alpha - \sin^2 \alpha) \left( \frac{\partial s}{\partial y'} \frac{\partial d^*}{\partial y'} - \frac{\partial s}{\partial x'} \frac{\partial d^*}{\partial x'} \right) \\ + 2 \sin \alpha \cos \alpha \left( \frac{\partial s}{\partial x'} \frac{\partial d^*}{\partial y'} + \frac{\partial s}{\partial y'} \frac{\partial d^*}{\partial x'} \right) + \text{c.c.} \end{aligned} \quad (86)$$

One can now derive and analyze the linearized field equations using the rotated coordinates  $(x', y')$  in exactly the same way as before, and the angle  $\alpha$  becomes just another variational parameter with respect to which the free energy is minimized. It turns out that it is possible to write down the linearized equations for  $s$  and  $d$  that are identical to Eqs. (45) with  $V$  changed to  $V = \epsilon_v (\hbar \omega_c / 2) (e^{2i\alpha} a^\dagger a^\dagger + e^{-2i\alpha} a a)$ . In such a case, one expects there will be a constant phase difference  $2\alpha$  between the  $s$  and  $d$  components, and the appropriate variational solution is of the form

$$\begin{aligned} d(x) &= e^{-i\alpha} [\varphi^+(x) + \varphi^-(x)], \\ s(x) &= e^{i\alpha} [\varphi^+(x) - \varphi^-(x)], \end{aligned} \quad (87)$$

where  $\varphi^+$  and  $\varphi^-$  are the normalized lowest eigenfunctions of a harmonic oscillator as defined by Eq. (49). The energy eigenvalue is easily evaluated, and we obtain a generalization of Eq. (51)

$$\frac{\langle E \rangle}{\Delta T} = \frac{T - T^*}{\Delta T} + \frac{1}{4} \left( \frac{\hbar \omega_c}{\Delta T} \right) \left[ (1 + \epsilon_v \cos^2 2\alpha) \tan \vartheta + (1 - \epsilon_v \cos^2 2\alpha) \frac{1}{\tan \vartheta} \right] - \frac{1}{2} \sqrt{\frac{2 \tan \vartheta}{1 + \tan^2 \vartheta}} \left[ 1 + \epsilon_v \sin^2 2\alpha \left( \frac{\hbar \omega_c}{\Delta T} \right) \frac{1 - \tan^2 \vartheta}{1 + \tan^2 \vartheta} \right]. \quad (88)$$

It is a simple matter to minimize  $\langle E \rangle$  with respect to  $\alpha$ , and one finds that minima can occur only for  $\alpha = 0, \pm \pi/2, \pm \pi$ . Thus we are led to the conclusion that within our variational solution the most stable vortex lattice is the one aligned with the underlying crystal as described above (cf. Fig. 11). Among the fourth order terms in the free energy only  $\beta_4(s^{*2}d^2 + s^2d^{*2})$  depends on  $\alpha$ . This dependence is particularly simple; upon rotation the constant  $\beta_4$  changes to  $\beta_4 \cos 4\alpha$ . Clearly, this term only has minima for trivial values of  $\alpha = 0, \pm \pi/2, \dots$ , so the above conclusion should hold even when the fourth order terms are included. In order to verify that this conclusion is not altered by some complicated interplay between angular dependencies of  $f_2$  and  $f_4$ , we have carried out the numerical minimization of the free energy of the rotated vortex lattice, along the lines indicated for the case  $\alpha = 0$ . We find that, for all the regions of parameter space that were investigated, the absolute minimum of the free energy occurs for  $\alpha = 0$ . As a consistency check we have also verified that identical minima are found for  $\alpha = \pm \pi/2, \pm \pi$ , which corresponds to the discrete rotations under the  $D_4$  group.

The above conclusion concerning the orientation of the vortex lattice may be understood by analyzing the mixed gradient term in the free energy density (1). Its structure forces the vortex lattice to align in such a way that the greatest gradient of order parameters is along one axis, while the smallest possible gradient is along the other axis. An arrangement of vortices such as the one shown in Fig. 11 definitely satisfies this requirement.

## V. SUMMARY AND DISCUSSION

The main goal of this work was to present a detailed study of the vortex state in a  $d$ -wave superconductor, focusing on the properties arising from  $s$ - $d$  mixing that have no analog in conventional superconductors. Analysis of the vortex state is done in two regimes: in the vicinity of  $H_{c1}$  where the properties of isolated vortex lines can be studied, and near  $H_{c2}$  where the collective properties of vortices forming a dense lattice are important.

For the single vortex line the topological structure of the induced  $s$ -wave order parameter is highly nontrivial, consisting of one counter-rotating unit vortex, centered at the core, surrounded by four additional positive vortices located symmetrically at a distance of several coherence lengths from the core. A result of this work is the realization that the above structure will occur for all parameter configurations that give rise to stable  $d$  wave in the bulk (provided one is well into the type-II regime), and not only in the vicinity of  $T_c$  as was originally suggested.<sup>18</sup> This conclusion is confirmed by an explicit integration of the GL equations over the wide range of parameters, and also by the calculations of Ichioka *et al.*,<sup>17</sup> who find analogous behavior using the quasiclassical Eilenberger equations. The question arises as to whether this

nontrivial topological structure of a single vortex could be probed experimentally. There are clearly many complicating factors which are likely to render this task very difficult. The main challenge arises from the fact that one expects the induced  $s$  component to be small, on the order of few percent of  $d$ . Such a small admixture of  $s$  might be hard to detect directly, and the corresponding distortion of the  $d$ -wave amplitude, supercurrent, and magnetic field distributions will also be small. It might in principle be possible to probe the  $s$  component by scanning Josephson tunneling from an  $s$ -wave tip, which by symmetry would not couple to the dominant  $d$  wave. With sufficient resolution such an experiment could detect strong anisotropy in the  $s$  component and possibly also the extra nodes. The internal structure of a vortex will also have an effect on the transport properties; e.g., it is conceivable that it may lead to changes in the Magnus force acting on a vortex in a current field. These issues clearly require further investigation.

Finally we note that although a finite induced  $s$ -component will restore the gap along the  $|k_x| = |k_y|$  directions in the vicinity of the core, this will not invalidate the prediction of Volovik<sup>10</sup> regarding the  $\sim \sqrt{H}$  contribution to the density of states (DOS) on the Fermi surface, which was recently confirmed by specific heat measurement by Moler *et al.*<sup>3</sup> Volovik's prediction is based on the observation (originally used by Yip and Sauls<sup>36</sup> to predict the nonlinear Meissner effect) that the quasiparticle excitation spectrum is shifted by the superfluid velocity field around the vortex core, with the dominant contribution coming from quasiparticles far from the core in position space and close to the nodes in momentum space. Since the amplitude of the  $s$  component far from the core vanishes as  $1/r^2$  the reduction of the DOS will be always negligible beyond a certain distance from the core compared to the energy shift due to superfluid velocity which decays only as  $1/r$ . Thus at relatively small fields compared to  $H_{c2}$ , such as were used in the specific heat measurements,<sup>3</sup> there will be no correction to the Volovik's result from the induced  $s$  wave. At stronger fields, when the vortices are closely spaced, corrections may appear; however, in such a case one expects Volovik's derivation to break down since the concept of an isolated vortex with a well defined asymptotic flow field loses its meaning in the dense Abrikosov lattice.

The vortex lattice near  $H_{c2}$  is in general oblique for a  $d$ -wave superconductor. The precise shape determined by an angle  $\phi$  between primitive vectors depends in a complicated way on the parameters in the GL free energy, most strongly on the mixed gradient coupling  $\epsilon_v$  and on magnetic field via the parameter  $\Lambda = \hbar \omega_c / \Delta T$ , which also determine the relative magnitude of  $s$ . Quite generally, when  $\epsilon_v = 0$ , the  $s$ -component vanishes and the lattice is triangular. By increasing  $\epsilon_v$  and  $\Lambda$  the lattice is continuously deformed, becoming oblique and eventually square. Observation of an

oblique flux lattice with  $\phi \approx 73^\circ$  was reported by Keimer *et al.*<sup>22</sup> using small angle neutron scattering from YBCO in magnetic fields  $0.5 \text{ T} \leq H \leq 5 \text{ T}$ . This would be in agreement with our result, although as was pointed out by Walker and Timusk,<sup>35</sup> the observed distortion may also be accounted for by the intrinsic  $a$ - $b$  plane anisotropy of the orthorhombic YBCO crystal. More recently an oblique vortex lattice with  $\phi \approx 77^\circ$  was found in YBCO using STM by Maggio-Aprile *et al.*<sup>23</sup> This technique also revealed elongated vortex cores with the ratio of principal axes about 1.5. If, as noted by authors, this elongation was due to the  $a$ - $b$  anisotropy in coherence lengths, within a simple London model of  $s$ -wave superconductivity this would lead to the flux lattice with an angle inconsistent with the actual observed value of  $77^\circ$ . Thus it would appear that the  $a$ - $b$  anisotropy alone cannot explain the observed distortion in the vortex lattice and additional effects, such as the internal symmetry of the order parameter, must be invoked in order to account for the experimental data. In this respect it would be most interesting to see if an oblique lattice can also be established experimentally in truly tetragonal superconductors. Alternatively it would be desirable to study the analogous GL theory for the  $D_2$  orthorhombic symmetry; unfortunately such a theory is complicated and contains even more phenomenological parameters so that a quantitative comparison with experiment would be difficult.<sup>37</sup> An alternative way of distinguishing between the effects of  $a$ - $b$  anisotropy and  $d$ -wave symmetry is to study the magnetic field distributions in the vortex lattice. The present theory predicts a double-peak structure in  $\mu$ SR or NMR line shapes whenever the flux lattice is oblique, while interpretations based on simple scaling arguments<sup>35</sup> lead to conventional single-peak line shapes.

#### ACKNOWLEDGMENTS

The authors are grateful to D. L. Feder, R. Joynt, M. Kvale, K. A. Moler, J. A. Sauls, M. Sigrist, and S. K. Yip for valuable discussions on the subject. This work has been partially supported by the Natural Sciences and Engineering Research Council of Canada, Ontario Centre for Materials Research, and by the National Science Foundation under Grant No. DMR-91-20361. We would also like to thank the Aspen Center for Physics, where this collaboration was initiated and part of the work was done.

#### APPENDIX: EVALUATION OF QUARTIC AVERAGES $\langle f_4 \rangle$ AND $\langle h_s^2 \rangle$

We first evaluate the contribution of  $\langle f_4 \rangle$ . For the purposes of calculation it is convenient to express  $\langle f_4 \rangle$  in terms of the functions  $\Psi_\pm$ ,

$$\begin{aligned} \langle f_4 \rangle = & \mu_1 \langle |\Psi_+|^4 \rangle + \mu_2 \langle |\Psi_+|^2 |\Psi_-|^2 \rangle + \mu_3 \langle |\Psi_+|^2 \Psi_+ \Psi_-^* \rangle \\ & + \mu_4 \langle \Psi_+^2 \Psi_-^{*2} \rangle + [\Psi_+ \leftrightarrow \Psi_-], \end{aligned} \quad (\text{A1})$$

where the constants  $\mu$  are given as follows

$$\begin{aligned} \mu_1 &= \frac{1}{16} (\beta_1 + \beta_2 + \beta_3 + 2\beta_4), \\ \mu_2 &= \frac{2}{16} (\beta_1 + \beta_2 - 2\beta_4), \\ \mu_3 &= \frac{4}{16} (-\beta_1 + \beta_2), \\ \mu_4 &= \frac{1}{16} (\beta_1 + \beta_2 - \beta_3 + 2\beta_4). \end{aligned} \quad (\text{A2})$$

The easiest way to evaluate the spatial averages is to express them as Fourier series. For example, one can write the typical member as follows:

$$\langle \Psi_+^{*2} \Psi_-^2 \rangle = \sum_{\mathbf{k}} \langle \Psi_+^* \Psi_- \rangle_{\mathbf{k}} \langle \Psi_+^* \Psi_- \rangle_{-\mathbf{k}}, \quad (\text{A3})$$

where we have used only the basic properties of the Fourier series. The utility of this formulation lies in the fact that components of the form  $\langle \Psi_\alpha^* \Psi_\beta \rangle_{\mathbf{k}}$  can be expressed in terms of simple Gaussians, and consequently the summations indicated in Eq. (A3) converge very rapidly. In particular it is useful to define

$$\langle \Psi_\alpha^* \Psi_\beta \rangle_{\mathbf{k}} = a_{\mathbf{k}} \Omega_{\alpha\beta}(\mathbf{k}), \quad (\text{A4})$$

where the coefficients  $a_{\mathbf{k}}$  are given by Eq. (78). The factors  $\Omega_{\alpha\beta}(\mathbf{k})$  contain all the dependence on the lattice structure and can be evaluated by explicit integration; we have

$$\begin{aligned} \Omega_{\alpha\alpha}(\mathbf{k}) &= \frac{1}{L_x} \exp \left\{ -\frac{l^2}{4} [(k_x/\sigma_\alpha)^2 + (k_y/\sigma_\alpha)^2] \right\}, \\ \Omega_{\alpha\beta}(\mathbf{k}) &= \frac{1}{L_x} \sqrt{\frac{2}{\sigma_+^2 + \sigma_-^2}} \exp \left\{ -\frac{l^2}{4} \frac{2}{\sigma_+^2 + \sigma_-^2} [k_x^2 + k_y^2 \right. \\ & \quad \left. + i(\sigma_\alpha^2 - \sigma_\beta^2) k_x k_y] \right\}, \quad \alpha \neq \beta. \end{aligned} \quad (\text{A5})$$

In terms of these functions,  $\langle f_4 \rangle$  can be written in a compact form,

$$\begin{aligned} \langle f_4 \rangle = & \sum_{\mathbf{k}} a_{\mathbf{k}} a_{-\mathbf{k}} \sum_{\alpha=\pm} [\mu_1 \Omega_{\alpha\alpha}^2(\mathbf{k}) + \mu_2 \Omega_{\alpha\alpha}(\mathbf{k}) \Omega_{\bar{\alpha}\bar{\alpha}}(\mathbf{k}) \\ & + \mu_3 \Omega_{\alpha\alpha}(\mathbf{k}) \Omega_{\alpha\bar{\alpha}}(\mathbf{k}) + \mu_4 \Omega_{\alpha\bar{\alpha}}^2(\mathbf{k})], \end{aligned} \quad (\text{A6})$$

which is suitable for numerical evaluation. In deriving Eq. (A6) we have used the symmetry  $\Omega_{\alpha\beta}(\mathbf{k}) = \Omega_{\alpha\beta}(-\mathbf{k})$  which is apparent from Eqs. (A5), and we use the notation  $\bar{\alpha} = -\alpha$ .

Let us now turn to calculation of  $\langle h_s^2 \rangle$ . A similar approach as above will work here if we write

$$\langle h_s^2 \rangle = \sum_{\mathbf{k}} h_s(\mathbf{k}) h_s(-\mathbf{k}). \quad (\text{A7})$$

The Fourier components  $h_s(\mathbf{k})$  can be deduced from Eq. (80),

$$\begin{aligned} h_s(\mathbf{k}) = & -\pi \delta \frac{e^* \hbar}{mc} [z_0 \langle |\Psi_+|^2 + |\Psi_-|^2 \rangle_{\mathbf{k}} \\ & + z_1 \eta_{\mathbf{k}} \langle |\Psi_+|^2 - |\Psi_-|^2 \rangle_{\mathbf{k}}], \end{aligned} \quad (\text{A8})$$

where we have introduced the quantity

$$\eta_{\mathbf{k}} = \begin{cases} \frac{k_x^2 - k_y^2}{k_x^2 + k_y^2}, & \text{if } \mathbf{k} \neq 0 \\ 0, & \text{if } \mathbf{k} = 0 \end{cases} \quad (\text{A9})$$

which allows all of the Fourier components of  $h_s(\mathbf{k})$  to be expressed by a single equation (A8). A compact expression for the average squared field can be written in terms of the functions  $\Omega_{\alpha\beta}(\mathbf{k})$  and has the following form:

$$\langle h_s^2 \rangle = \pi^2 \delta^2 \left( \frac{e^* \hbar}{mc} \right)^2 \sum_{\mathbf{k}} a_{\mathbf{k}} a_{-\mathbf{k}} [(z_0 + z_1 \eta_{\mathbf{k}}) \Omega_{++}(\mathbf{k}) + (z_0 - z_1 \eta_{\mathbf{k}}) \Omega_{--}(\mathbf{k})]^2. \quad (\text{A10})$$

Let us finally write, for the purpose of completeness, the expression for the average field:

$$\begin{aligned} \langle h_s \rangle &\equiv h_s(\mathbf{k}=0) = -\pi \delta z_0 a_0 \left( \frac{e^* \hbar}{mc} \right) [\Omega_{++}(0) + \Omega_{--}(0)] \\ &= -2\pi \delta \frac{z_0}{L_x} \left( \frac{e^* \hbar}{mc} \right) (|c_0|^2 + |c_1|^2). \end{aligned} \quad (\text{A11})$$

We have now expressed all the averages that are needed to minimize the Gibbs free energy (68). In principle, both

$\beta_A$  and  $\kappa$  can now be evaluated numerically using the rapidly converging sums (A6) and (A10). However, following the work of Kleiner, Roth, and Autler,<sup>21</sup> it is practical to carry out the minimization with respect to the constants  $c_0$  and  $c_1$  analytically. This reduces the relevant parameter space to a single parameter, the geometric ratio  $R = L_x/L_y$ . To this end we have purposely singled out the dependence on these parameters in the expressions for  $\langle f_4 \rangle$  and  $\langle h_s^2 \rangle$ . In particular, the entire dependence on  $c_0$  and  $c_1$  is contained in the constants  $a_{\mathbf{k}}$ , and both  $\langle f_4 \rangle$  and  $\langle h_s^2 \rangle$  are of the form

$$\begin{aligned} &\sum_{\mathbf{k}} a_{\mathbf{k}} a_{-\mathbf{k}} f(k_1, k_2) \\ &= \sum_{k_1 k_2} \{ e^{i\frac{\pi}{2} k_1 k_2} [c_0 c_{k_2}^* + (-1)^{k_1} c_1 c_{k_2+1}^*] \}^2 f(k_1, k_2), \end{aligned} \quad (\text{A12})$$

where  $f(k_1, k_2)$  is independent on  $c_0$  and  $c_1$ . Our goal here is to factor out the entire dependence of this expression on the constants  $c_0$  and  $c_1$ . This is done by considering separately the cases when  $k_1, k_2$  are even and odd, and recalling that by assumption  $c_{2k} = c_0$  and  $c_{2k+1} = c_1$ . We obtain an expression of the following form:

$$\begin{aligned} &(|c_0|^4 + |c_1|^4) \sum_{k_1 k_2} [f(2k_1, 2k_2) + f(2k_1 + 1, 2k_2)] + (c_0^2 c_1^{*2} + c_0^{*2} c_1^2) \sum_{k_1 k_2} [f(2k_1, 2k_2 + 1) - f(2k_1 + 1, 2k_2 + 1)] \\ &+ 2|c_0|^2 |c_1|^2 \sum_{k_1 k_2} [f(2k_1, 2k_2) - f(2k_1 + 1, 2k_2) + f(2k_1, 2k_2 + 1) + f(2k_1 + 1, 2k_2 + 1)]. \end{aligned} \quad (\text{A13})$$

Clearly, the entire denominator  $8\pi \langle f_4 \rangle - \langle h_s^2 \rangle$  of the free energy (66) can be written in the above form, where the dependence on constants  $c_0$  and  $c_1$  is explicitly shown. Combining this with the expression (A11) for the average induced field  $\langle h_s \rangle$  it is easy to see that the total free energy (66) can be written schematically as

$$-\frac{(|c_0|^2 + |c_1|^2)^2}{(|c_0|^4 + |c_1|^4) G_0(R) + 2|c_0|^2 |c_1|^2 G_1(R) + 2\text{Re}(c_0^2 c_1^{*2}) G_2(R)}, \quad (\text{A14})$$

where  $G_i(R)$  are complicated functions of  $R$  and other GL parameters, but are independent of  $c_0$  and  $c_1$ . The above expression can be easily minimized with respect to  $c_0$  and  $c_1$ ; one obtains that a condition for the minimum is  $c_1 = \pm i c_0$ . Clearly, the value of the expression (A14) only depends on the ratio  $c_1/c_0$ , so we can arbitrarily choose

$$c_0 = 1, \quad c_1 = i. \quad (\text{A15})$$

With this choice, we have an identity

$$a_{\mathbf{k}} a_{-\mathbf{k}} = [(-1)^{k_1} + (-1)^{k_2}]^2, \quad (\text{A16})$$

which will simplify evaluation of the sums in  $\langle f_4 \rangle$  and  $\langle h_s^2 \rangle$ . Also, the expression for the average induced field (A11) simplifies:

$$\langle h_s \rangle = -4\pi \delta \frac{z_0}{L_x} \left( \frac{e^* \hbar}{mc} \right). \quad (\text{A17})$$

- <sup>1</sup>For a review, see D. J. Van Harlingen, *Rev. Mod. Phys.* **67**, 515 (1995).
- <sup>2</sup>D. A. Wollman, D. J. Van Harlingen, W. C. Lee, D. M. Ginsberg, and A. J. Leggett, *Phys. Rev. Lett.* **71**, 2134 (1993); D. A. Brawner and H. R. Ott, *Phys. Rev. B* **50**, 6530 (1994); C. C. Tsuei, J. R. Kirtley, C. C. Chi, L. S. Yu-Jahnes, A. Gupta, T. Shaw, J. Z. Sun, and M. B. Ketchen, *Phys. Rev. Lett.* **73**, 593 (1994); A. Mathai, Y. Gim, R. C. Black, A. Amar, and F. C. Wellstood, *ibid.* **74**, 4523 (1995).
- <sup>3</sup>K. A. Moler, D. J. Baer, J. S. Urbach, R. Liang, W. N. Hardy, and A. Kapitulnik, *Phys. Rev. Lett.* **73**, 2744 (1994).
- <sup>4</sup>A. Maeda, Y. Iino, T. Hanaguri, K. Kishio, and T. Fukase, *Phys. Rev. Lett.* **74**, 1202 (1995).
- <sup>5</sup>J. Ma, C. Quitman, R. J. Kelley, H. Bergen, C. Margaritondo, and M. Onellion, *Science* **267**, 862 (1995); H. Ding, J. C. Campuzano, and G. Jennings, *Phys. Rev. Lett.* **74**, 2784 (1995).
- <sup>6</sup>P. Chaudhari and S.-Y. Li, *Phys. Rev. Lett.* **72**, 1084 (1994).
- <sup>7</sup>A. G. Sun, D. A. Gajewski, M. B. Maple, and R. C. Dynes, *Phys. Rev. Lett.* **72**, 2267 (1994).
- <sup>8</sup>J. Bertouras and R. Joynt, *Europhys. Lett.* **31**, 119 (1995).
- <sup>9</sup>M. Sigrist and T. M. Rice, *Z. Phys. B* **68**, 9 (1987).
- <sup>10</sup>G. E. Volovik, *Pis'ma Zh. Éksp. Teor. Fiz.* **58**, 457 (1993) [*JETP Lett.* **58**, 469 (1993)].
- <sup>11</sup>P. I. Soininen, C. Kallin, and A. J. Berlinsky, *Phys. Rev. B* **50**, 13 883 (1994).
- <sup>12</sup>R. Joynt, *Phys. Rev. B* **41**, 4271 (1990).
- <sup>13</sup>P. Kumar and P. Wofle, *Phys. Rev. Lett.* **59**, 1954 (1987).
- <sup>14</sup>M. M. Doria, H. R. Brand, and H. Pleiner, *Physica C* **159**, 46 (1989).
- <sup>15</sup>Y. Ren, J. H. Xu, and C. S. Ting, *Phys. Rev. Lett.* **74**, 3680 (1995).
- <sup>16</sup>Y. Wang and A. H. MacDonald, *Phys. Rev. B* **52**, R3876 (1995).
- <sup>17</sup>M. Ichioka, N. Enomoto, N. Hayashi, and K. Machida (unpublished); (private communication).
- <sup>18</sup>A. J. Berlinsky, A. L. Fetter, M. Franz, C. Kallin, and P. I. Soininen, *Phys. Rev. Lett.* **75**, 2200 (1995).
- <sup>19</sup>The authors of Ref. 16 studied the electronic structure of the vortex lattice. They found that in the parameter region they were concerned with, the triangular lattice had a lower free energy than the square lattice. Since they did not explicitly consider oblique lattices, their result does not contradict our work.
- <sup>20</sup>A. A. Abrikosov, *Zh. Éksp. Teor. Fiz.* **32**, 1442 (1957) [*Sov. Phys. JETP* **5**, 1174 (1957)].
- <sup>21</sup>W. H. Kleiner, L. M. Roth, and S. H. Autler, *Phys. Rev.* **133**, A1266 (1964).
- <sup>22</sup>B. Keimer, J. W. Lynn, R. W. Erwin, F. Dogan, W. Y. Shih, and I. A. Aksay, *J. Appl. Phys.* **76**, 6788 (1994).
- <sup>23</sup>I. Maggio-Aprile, Ch. Renner, A. Erb, E. Walker, and Ø. Fischer, *Phys. Rev. Lett.* **75**, 2754 (1995).
- <sup>24</sup>Within the GL theory the sign of  $\gamma_v$  is unimportant as the change  $\gamma_v \rightarrow -\gamma_v$  and the simultaneous interchange of the  $x$  and  $y$  coordinate axes leaves the free energy (1) invariant. The sign of  $\gamma_v$  becomes of importance when making contact with microscopic models which describe internal fermionic degrees of freedom of pairs. On this level the internal structure causes the  $d$ -wave order parameter to change sign under  $\pi/2$  rotations. In this respect our convention implies  $\Delta_d(\mathbf{r}, \mathbf{k}) = \Delta_d(\mathbf{r})(\cos k_y - \cos k_x)$  for  $\Delta_d(\mathbf{r}) > 0$  in the uniform system, in which case our choice of  $\gamma_v > 0$  is consistent with the prediction of the continuum weak coupling theory (Ref. 15).
- <sup>25</sup>R. Micnas and J. Ranninger, *Rev. Mod. Phys.* **62**, 113 (1990).
- <sup>26</sup>M. Tinkham, *Introduction to Superconductivity* (Krieger, Malabar, 1975).
- <sup>27</sup>This result is at variance with the claim of Ren *et al.* (Ref. 15) who find that  $s$  and  $d$  exhibit the same leading temperature dependence. However more recent numerical calculations of the same group (Ref. 29) seem to find that  $s$  decays faster than  $d$  near  $T_d$ , in agreement with our result.
- <sup>28</sup>The winding number (or vorticity) is defined in the conventional way (Ref. 26) as  $n_v = (1/2\pi)\oint_C \nabla \vartheta \cdot d\mathbf{l}$ , where  $\vartheta$  is the phase of the order parameter and  $C$  is an arbitrary closed contour containing the vortex.
- <sup>29</sup>J. H. Xu, Y. Ren, and C. S. Ting (unpublished).
- <sup>30</sup>P. I. Soininen and N. B. Kopnin, *Phys. Rev. B* **49**, 12 087 (1994).
- <sup>31</sup>G. H. Golub and C. F. Van Loan, *Matrix Computations* (Johns Hopkins University Press, Baltimore, 1989).
- <sup>32</sup>Note that within this scheme one should in principle add one more variational parameter  $\alpha$  by allowing  $\varphi^+$  and  $\varphi^-$  to enter the definition of  $s$  and  $d$  in Eq. (46) with different weights, i.e.,  $d = \varphi^+ \cos \alpha + \varphi^- \sin \alpha$ , etc. A careful analysis of this case shows that  $E$  is always minimized by  $\alpha = \pi/4$ , thus recovering Eq. (46).
- <sup>33</sup>Y. Hidaka, Y. Enomoto, M. Suzuki, M. Oda, and T. Murakami, *Jpn. J. Appl. Phys.* **26**, L377 (1987).
- <sup>34</sup>T.K. Worthington, W.J. Gallagher, and T.R. Dinger, *Phys. Rev. Lett.* **59**, 1160 (1987).
- <sup>35</sup>M. B. Walker and T. Timusk, *Phys. Rev. B* **52**, 97 (1995).
- <sup>36</sup>S. K. Yip and J. A. Sauls, *Phys. Rev. Lett.* **69**, 2264 (1992).
- <sup>37</sup>We have verified by an explicit calculation that adding second order invariants appropriate for the orthorhombic symmetry to the free energy does not qualitatively alter our conclusions regarding the vortex lattice.